Author comments on "Causes of interannual variability of tropospheric ozone over the Southern Ocean" by Junhua Liu et al.

We thank the two reviewers for their comments. Both of them recommend publication with minor revisions. We have addressed all comments in detail below and have clarified the text in the relevant sections.

In the following, we address the concerns raised by both reviewers. Reviewers' comments are italicized.

Anonymous Referee #1
Received and published: 14 November 2016
The manuscript of Liu et al. discusses the interannual variability of tropospheric ozone over regions where the southern tropospheric ozone maximum is found. This is a well-established feature of tropospheric composition, though such a systematic exploration of its interannual variability in different horizontal and vertical regions, and with a focus on exploring the role of different drivers has not been pursued before. The manuscript is certainly within the scope of ACP, it is generally well written, and the findings will be useful for the understanding of tropospheric ozone variability further. I recommend its publication following some (mostly minor) suggested modifications described below.

GENERAL COMMENT:
1: I find the second part of the title misleading. The Southern Ocean is mentioned, but this Ocean's northernmost limit is usually taken as 50 or 60S, which is far from where the focus of this study lies. I suggest modifying possibly to "Causes of interannual variability over the southern hemispheric tropospheric ozone maximum".

The title has been modified as suggested in the revised manuscript.

SPECIFIC COMMENTS:
2: Page 2, Line 30: What is special about September, leading to the "even during September" statement. It is not clear at this stage.

September is the month that CO has the largest contribution from southern hemispheric biomass burning. We deleted 'even during September' to make the context clear.

3: Page 2, Line 39: Suggest changing to "especially in the upper troposphere".
The text has been modified as suggested

4: Figure 1: Define "upper tropospheric" in the caption.
The definition of "upper tropospheric" has been added in the caption.

5: Page 4, Line 81: Also, Voulgarakis et al. (2011) demonstrated that between transport processes, it is the STE that is the key driver following El Niño events. It is also worth mentioning somewhere in the introduction that Hess and Mahowald (2009), who prescribed stratospheric ozone, found that IAV of ozone at 500hPa did not show features *similar to the Southern Hemisphere ozone maximum described here (see their Fig. 2 & 3), possibly implying the important role of the stratosphere.*

These two references have been added in the text. Please see below:

Voulgarakis et al. (2011) demonstrated that increases in the amounts of stratospheric ozone entering the troposphere following El Niño events are mainly driven by changes in the STE.

Hess and Mahowald (2009) used a CTM to quantify relative interannual variability in global model ozone in hindcast simulations with constant emissions and prescribed stratospheric ozone. The CTM was driven by two sets of meteorological fields: a) the National Center for Environmental Prediction/National Center for Atmospheric Research reanalysis; b) from a simulation using the Community Atmosphere Model (CAM-3) forced with observed sea surface temperatures. Their study found that relative IAV of ozone at 500 hPa shows the maximum between the Equator and 30S in JJA and DJF.

6: Page 5, Line 121: Please change "section" to "Section", as there is only one Section 3.
The text has been modified as suggested.

7: Page 5, Line 129: Gap after http:// not needed.
The text has been modified as suggested.

8: Page 5, Line 130: Same amount of levels after re-gridding?
Yes, the vertical levels remain unchanged. The text has been modified as: we regrid it to 2°x2.5° horizontal grid for input to the GMI-CTM simulations in this study.

9: Page 6, Line 136: Please check end of sentence and amend.
The text has been modified.

10: Page 6, Lines 142-145: Emissions are important, since their role is investigated, so there needs to be an at least brief mention of what they are here. A quick mention of the reference is not enough.

The text has been modified as below:

The GMI-CTM standard simulation (labeled as Hindcast-VE) used in this study for 1992-2011 includes monthly and inter-annually varying emissions with anthropogenic, biomass burning, and biogenic sources. Anthropogenic emissions are based on the EDGAR 3.2 Inventory (Olivier et al., 2005), overwritten with available regional inventories for North America, Europe, Asia and Mexico. More details are given in Strode et al. (2015). Biomass burning emissions are from the Global Fire Emission Database, GFED3 (van der Werf et al., 2010). Emission before 1997 are obtained from GFED3 emission climatology averaged for 2001 to 2009 applied with regional-scale IAV, which was derived from satellite information on fire activity (ATSR) and/or aerosol optical depths from the Total Ozone Mapping Spectrometer (TOMS) by Duncan et al. (2003). Biogenic emissions of isoprene and monoterpenes follow the latest version of the MEGAN algorithm (Guenther et al., 2006). Besides the standard simulation, we carry out a control run with anthropogenic and biomass emissions fixed at year 2000 levels. The comparison between the control and standard simulation allows us to quantify effects of emission IAV on ozone IAV.

Also: Why was specifically 2000 used for the fixed emissions simulation? Any implications of this selection?

Year 2000 is about the middle point of examined period (1991-2011). However, the selection of year with constant emission does not affect the conclusion of how emission IAV affects the ozone IAV.

11: Page 6, Line 148: Mention the global total of lightning emissions again. In fact, this is where the more detailed description of what was used for lightning belongs.

We moved the lightning description in the Introduction Section to here as below:
In our GMI-CTM, the lightning parameterization follows the scheme described by Allen et al (2010). The regional lightning NO_X emission, calculated online by coupling to the deep convective transport in the model, varies from year to year. The global total of NO_X from lightning is fixed at 5.0 TgN/yr.

12: Page 6, Line 151-153: Do they vary with time (e.g. are there any trends in CFCs and N2O, which would affect ozone)?

Yes, both CFCs and N_2O have trends. CFCs increase before 1999 then decrease after 1999. N_2O shows an increasing trend through the study period. The trend in stratospheric ozone due to CFCs and N_2O during the period of interest is small compared with IAV in stratospheric ozone input to the troposphere. Meanwhile, in this study, we examined the effect of IAV of ozone input from stratosphere on the IAV of tropospheric ozone using the $StratO_3$ tracer. The variations of the contribution from stratospheric ozone could result from the variation in stratospheric ozone (which is relate to variations in CFCs and N_2O) or the changes in STE or both. We did not separate these effects in our study. Further examination of their separate effects is beyond the scope of this paper.

13: Page 6, Line 157: They are both artificial, so please specify that you are referring to e90 (i.e. "The e90 tracer is...").
The text has been modified as suggested.

14: Page 7, Line 168: Why is higher resolution used in this simulation?
We did our analysis using the highest resolution that available in our simulations.

15: Page 9, Line 230: Not clear how the Walker circulation affects the meridional structure of stratospheric ozone contribution, given that the WC occurs in the zonal

direction. Maybe the authors mean that the zonal (and not the meridional) variations in the southernmost extent are driven by the WC?
Two places in this paragraph have been changed into 'zonal circulation'.

16: Page 9, Lines 235-237: It is not clear what is suggested here. For ozone in the tropics to be associated with StratO3, I would think that the upper and lower panels of Fig. 2 should have a resemblance in the tropics. That is not something obvious on the figure. Moreover, how can one see an ozone minimum in the three regions mentioned from Figure 2 (upper panel)?

We modified the text as suggested in places where clarification was needed. Please see line 259-272 in the modified manuscript.

The bottom panel of Figure 2 suggests the regions with minimum stratospheric ozone contribution in the tropics reaches further south over Indian Ocean than the tropical eastern Pacific and Atlantic. The zonal variation of stratospheric contribution in the tropics is in agreement with that of ozone as shown in the upper panel of Figure 2, showing elevated ozone over the tropical eastern Pacific and Atlantic and the minimum over Indian Ocean.

17: Page 9, Lines 241-242: The Southern Ocean is mentioned, but this Ocean's northernmost limit is usually taken as 50 or 60S, which is far from where the stratospheric influence is found. I suggest changing to "southern Indian and Pacific Oceans".
The text has been modified as suggested.

18: Page 9, Lines 248-251: Please explain why the southern Pacific was not also selected for study.

We did not select southern Pacific is because: although tropospheric ozone is elevated over this region, it does not reach the regional maximum. The ozone concentration in this region is lower than that in southern Atlantic and southern Indian Ocean. We did a similar analysis on controlling factors of tropospheric ozone over the southern Pacific. Our results suggest that stratospheric ozone input playing a dominant role on the IAV of tropospheric ozone over southern Pacific.

19: Page 10, Lines 254-256: It would have been nice to show a simple map with IAVs. Similar to Fig. 1, but for IAV (e.g. standard deviation divided by the mean). It would give an immediate first view of where the "hot-spots" of variability are, both for certain levels and for UTOC.
We added Figure R1 into modified manuscript as Figure 3.

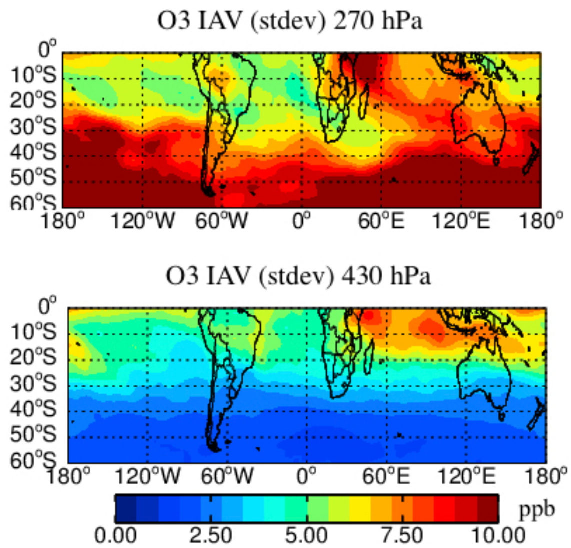

Figure R1: The IAV of simulated ozone at 270 hPa (top) and 430 hPa (bottom). The IAV is represented by the standard deviation of ozone anomalies (removing the monthly mean) over 1991-2011. Stronger ozone IAV happens over subtropical south Atlantic and subtropical south Indian Ocean at 270 hPa. At 430 hPa, Tropical southeastern Pacific and tropical South Atlantic has slightly larger IAV.

20: Figure 3: Why only from 2005 to 2011 and not for the entire period? Also: The labeling of the x-axis could be made more simple/clear.
We modified the x-label for Figure 4 and 5 in the revised manuscript. Aura data are only available since late 2004.

21: Page 10, Lines 258-259: This sentence needs to be moved to the caption, to make clear what is meant by "anomalies".
This sentence has been added to the caption.

22: Figures 3 & 4: I think "and upper tropospheric ozone column (UTOC, integrated from 500 hPa to the tropopause) anomalies" should be moved earlier in the sentence. Page 11, Lines 284-285: It would be clearer with IAV maps - as I described above - which areas show larger or smaller IAV.
We modified the figures and captions to show tropospheric column situation first.
For Line 284-285, we modified the text to be precise.

23: Page 12, Lines 318-321: Why are the authors mentioning this? Perhaps to suggest that this mechanism is probably responsible for the larger IAV in S. Atl. mentioned earlier, even though IAV in African emissions is small (i.e. there is a remote effect). Please clarify. Also: Perhaps use a clearer term instead of "eastern regions". I believe this is not a standard term. At the very least you can define its borders in this sentence *rather than later. Or perhaps use "South and Southeast Asia"? BTW: The later definition on lines 324-325 does not seem to include Australia.*

Emissions from South and Southeast Asia affect the southern hemisphere along with emissions from Africa and South America. We therefore include this region in our discussion.

The larger IAV in S. Atlantic results from the larger IAV from South America biomass burning.

We clarified the definition of eastern region in the text and replaced the eastern region with 'South and Southeast Asia" both in text and figure.

24: Page 12, Line 340: Where do those percentages of variability "explained" come from?
These are calculated from the correlations shown in the figure 7 in the revised manuscript.

25: Page 13, Line 368: "great" -> "greater".

The text has been modified as suggested.

26: Page 13, Line 369: Paragraph too long. Maybe break it here.
The paragraph has been modified as suggested.

27: Page 14, Line 391: What does a negative response to ENSO mean here? To the ENSO index?

We replaced the "ENSO" with "the Niño 3.4 index".

28: Page 15, Lines 417-418: From the figure it seems that the "eastern region" is the largest contributor, no?

The discussion here is for the situation at 430 hPa in September, which is the left bottom panel of Figure 12 in the revised manuscript. The emissions from S. America and southern Africa are the larger emission contributors at 430 hPa in September. In the next few lines, we mentioned that emission from South and Southeast Asia is the largest contributor in December at both levels.

29: Page 16, Line 443: "lightning activities" -> "lightning activity".
The text has been modified as suggested.

30: Page 16, Line 455: "NOX" -> "NOx".
The text has been modified as suggested.

31: Page 17, Line 475: Somewhat vague statement. Deep convection transports (mixes up) ozone-poor air from near the surface to the UT.

The text has been modified. Please see below.
Deep convection over a clean region reduces upper tropospheric ozone by mixing up ozone-poor air from near the surface. This effect could be opposite if deep convection happens over a polluted region with relatively high ozone and its precursors (Lawrence et al., 2003; Ziemke, et al., 2015).

32: Page 19, Lines 549-550: Suggest rephrasing to "The stratospheric contribution is still significant at 430 hPa, but drops to less than half of that at 270 hPa".
The text has been modified as suggested.

33: Page 20, Line 564: Also in Young et al. (2013) (see their Fig. 3).
The reference has been added as suggested.

34: Page 20, Lines 569-570: Suggest rephrasing to "to the radiative forcing of climate".
The text has been modified as suggested.

Interactive comment on "Causes of interannual variability of tropospheric ozone over the Southern Ocean" by Junhua Liu et al.

Anonymous Referee #2
Received and published: 12 December 2016
Review of Liu et al., Causes of interannual variability of tropospheric ozone over the Southern Ocean

The manuscript by Liu et al. presents an analysis of a series of runs with the Global Modelling Initiative (GMI) CTM driven by MERRA re-analysis to look at the inter-annual variability of ozone in the middle to upper troposphere in regions of the southern hemisphere. To investigate the contribution of stratospheric input on ozone, a diagnostic tracer of stratospheric ozone is included. To estimate the role of inter-annual variability in emissions, the difference between the full simulation and a simulation with constant emissions is used. Multiple linear regression and correlations are used to estimate the contribution of these influences on the year-to-year variability in the model ozone. The study finds a significant contribution of the stratosphere to ozone variability in the upper troposphere, even deep into the tropics, a finding that furthers our evolving understanding of the significant role stratospheric input can have on ozone in the troposphere.

The paper is well written and clearly presents a well thought out analysis. I do not have any significant concerns with the material presented.
1: My one methodological concern is the approach to quantify the contribution of stratospheric ozone (stratO3) and the interannual variability in ozone precursor emissions (emissO3). For example, for the South Atlantic region Figure 6 presents the multiple linear regression (MLR) of stratO3 and emissO3 against the model ozone anomaly. The combination of these two factors can reproduce a high degree of the interannual variability of the model ozone, up to nearly 76% for December at 270 hPa. To separate the contribution of stratO3 and emissO3, the correlation of the stratO3 term from the MLR against the original model ozone timeseries is calculated. Then the contribution of emissO3 is calculated from the correlation of the emissO3 term against the residual that results from removing the stratO3 contribution. During the original MLR analysis the stratO3 and emissO3 terms were simultaneously fitted to the ozone anomaly, but the contribution of stratO3 and emissO3 is calculated by correlation sequentially. The end result is that while the combined stratO3/emissO3 regression explains 76% of the variance for December at 270 hPa (Figure 6), individually stratO3 accounts for 61% and emissO3 accounts for 40% (Figure 7).
Given the process of simultaneously fitting the stratO3 and emissO3 terms during the MLR, is not the correct way to calculate their individual contributions to regress these terms individually against the original timeseries? I would argue that if correlation of stratO3 accounts for 61% of the variance, then emissO3 should account for approximately 15% since the combination of the two accounts for 76%. The process seems to work in the extreme where one component explains all of the variance – the south Atlantic at 270 hPa in August, for example – but for cases where both components contribute substantially the approach of regressing the second term against the residual

seems to give an inflated estimate. This could be because the process of calculating the residual by removing the contribution from the first term has also removed a large fraction of the variance? And since there is no correct order to which of the two terms is fitted first and which is fitted second, they both should be correlated against the same (original) timeseries. Following this approach one could argue that emissO3 explains a certain fraction of the residual variance, but one could not directly compare the stratO3 and emissO3 correlations.
The change in methodology argued for above may have some impact on the conclusion of the relative importance of stratO3 and emissO3 for certain regions at certain times but I do not see how it would fundamentally alter the conclusions of the paper.

Thanks a lot for the reviewer's comments on this issue. We agree with the comments and modified the calculated as suggested.

Considering that the regressors (StratO_3, EmisO_3, lightningNOx) might be correlated and not orthogonal with each other, we estimate the amount of variance explained by each regressor following the method described in (Kruskal, 1987;Chevan and Sutherland, 1991; Groemping, 2007). In this method, regressor is added to the model one by one and the corresponding sequential sum of squares for each regressor is calculated. The sequential sum of squares depends on the regressors already in the model; we therefore do the calculation for every possible order in which regressors can enter the model, and then average over orders. Below are two examples of variance table.
1) The first one is for the multi-regression with two regressors

Table 1: Analysis of variance for regression with StratO_3 and EmisO_3 over South Atlantic in December at 270 hPa.

Source	SS
Regression	135.94
Error	45.47
Total	181.41
Variance by regression	0.75

Sequential sum of square

Source	Seq SS (StraO3)	Seq SS (EmisO3)
StratO3 + EmisO3	110.81	25.13
EmisO3 + StratO3	59.29	76.65
Source	StratO3	EmisO3
Mean SS	85.05	50.89
Variance explained	0.47	0.28

2) The second one is for the multi-regression with three regressors (StratO_3, EmisO_3, and lightning NOx) over tropical Atlantic in September at 270 hPa

Table 2: Analysis of variance table for regression with $StratO_3$, $EmisO_3$ and lightning NOx over Tropical Atlantic in September at 270 hPa.

Source	SS
Regression	210.05
Error	108.98
Total	319.03
Variance by regression	0.66

Sequential sum of square

Source	Seq SS ($StraO_3$)	Seq SS ($EmisO_3$)	Seq SS (lightningNOx)
$StratO_3$ + $EmisO_3$ + LightningNOx	167.25	7.02	35.78
$StratO_3$ + LightningNOx + $EmisO_3$	167.25	0.88	41.92
$EmisO_3$ + $StratO_3$ + LightningNOx	156.08	18.19	35.78
$EmisO_3$ + LightningNOx + $StratO_3$	112.90	18.19	78.96
LightningNOx + $StratO_3$ + $EmisO_3$	114.24	0.88	94.94
LightningNOx + $EmisO_3$ + $StratO_3$	112.90	2.21	94.94
Source	$StratO_3$	$EmisO_3$	Lightning NOx
Mean SS	138.44	7.90	63.72
Variance explained	0.43	0.03	0.20

We modified the discussion in the text. The changes in methodology discussed above have impact on the value of the relative contributions of $stratO_3$ and $emissO_3$ for certain regions at certain times, but the conclusion of relative importance does not change.

My other comments are mostly minor and related to specific parts of the paper. They are detailed below.

2: Lines 103-104. A minor quibble that part of the treatment of lightning NOx is discussed here, where it is stated that the global total is fixed at 5 Tg-N/year, and part is discussed at Lines 146-148. It would help the reader to rework a bit these two parts to combine them in one place.

The text has been modified. Please see our response to question 11 of reviewer 1

3: Lines 103-104. If lightning NOx emissions are held constant, how do you derive the interannual variability in lightning NOx that is used in the correlation shown in Figure 14. It must be the variability over a particular region, but I am not sure I found where that is discussed.

In the modified manuscript, we mentioned how regional lightning NOx is calculated online. Please see below: The regional NO_X emission from lightning is calculated online by coupling to the deep convective transport in the model and varies from year to year.

4: Lines 143-145. I guess it is obvious that the run with constant emissions fixed at the year 2000 levels means that the annual cycle of year 2000 emissions repeats. Sorry for another quibble, but it would help remove any doubt if the wording were more explicit.
Yes. The text has been modified for clarification.

Besides the standard simulation, we carry out a control run with anthropogenic and biomass emissions hold at year 2000 level with seasonality.

5: Lines 159 - 162. Here the stratO3 tracer is discussed. When it is stated that the stratO3 tracer is 'removed in the troposphere with the same loss frequency…' is that the same loss frequency as Ox and how exactly is Ox defined? Would you know the global average tropospheric O3 lifetime that you would derive from the loss frequency you used for stratO3?

The stratosphere O_3 is the same with daily output of the respective full chemistry run. The tropopause is defined as e90 tracer to be 75 ppb. The three chemical loss rates in the troposphere are archived from monthly full chemistry run.
$O_1D + H_2O = 2\ OH$
$HO_2 + O_3 = 2\ O_2 + OH$
$OH + O_3 = HO_2 + O_2$
The $StratO_3$ was removed at the surface level, which is equal to the dry deposition process. There is no chemical production of $StratO_3$ in the troposphere.

6: Line 222 . '…represents [the] fraction of tropospheric ozone from [the] stratosphere…'

The text has been modified as suggested.

7: Line 237. I would suggest removing 'of' from 'Within the Atlantic, despite of the…'
The text has been modified as suggested.

8: Lines 259 – 261. Here it is mentioned that the interannual variability in the GMI simulation is larger than in the GMAO assimilated ozone for the two tropical regions. Is there any additional information that could be provided as to why this may be the case? Perhaps some comparisons from the Wargan et al. (2015) paper against independent observations or the role of emissions in the assimilation that is mentioned at Lines 277-279? This would seem to be an important component of the comparison if one is to have confidence in the analysis of interannual variability presented later in the paper.

There are limitations in the assimilation data including 1) No chemistry and lack of emissions in the troposphere in the assimilation, 2) no direct observational constraint in the troposphere. Both could contribute to the less IAV in the GMAO assimilated data at one pressure level in the troposphere, especially in the middle and lower troposphere. For the upper tropospheric column comparison, the agreement in the magnitude of IAV between GMI simulation and GMAO assimilated data improves.

9: Lines 367 – 369. The statement on the relative contribution of emissions to ozone variability at 270 and 430 hPa will probably need to be revisited if the method of attribution is revised as argued for above.
Please see our response to question 1 above.

10: Lines 454-456. On Figure 12, it would be interesting to see the same fit of ozone with lightning at 430 hPa as is shown for 267 hPa.
With the source originated from the upper troposphere, the lightning NOx has the largest effect in the upper troposphere and the effects are insignificant at 430 hPa. We therefore did not show the comparison at 430 hPa.

11: Line 484-485. 'Figure 14 compares the model residual after removing the contributions from StratO3 and EmissO3…' and I would raise the same concern that the analysis is overestimating the contribution of lightning to explaining the variance in ozone.
Please see our response to question 1 above.

Lines 552 – 556. Because the correlation of lightning with ozone variability is negative, the authors suggest deep convection is having a negative effect on ozone in the upper troposphere by lofting clean surface air. I agree that could definitely be a possibility, but can you rule out that the correlation is signalling some other effect? Perhaps circulation changes that are associated with the interannual variability in deep convection?

We cannot rule out other possibilities. The reason we focus on convection effects is that in the model, the lightning parameterization is coupling to the deep convective transport. Increase in deep convection produces more upper tropospheric NOx from lightning, which results more ozone production. On the other hand, deep convection could decrease the upper tropospheric ozone by mixing up ozone-poor air from surface. Therefore, the convection has two opposite but quite important and direct effects on upper tropospheric ozone.

Lines 825-829. The colour scale on Figure 1 indicates it is ppb and it should be DU as I understand it.
We modified the unit for color bar.

Reference:
Allen, D., Pickering, K., Duncan, B., and Damon, M.: Impact of lightning NO emissions on North American photochemistry as determined using the Global Modeling Initiative (GMI) model, Journal of Geophysical Research-Atmospheres, 115, 10.1029/2010jd014062, 2010.

Chevan, A., and Sutherland, M.: HIERARCHICAL PARTITIONING, American Statistician, 45, 90-96, 10.2307/2684366, 1991.

Duncan, B. N., Martin, R. V., Staudt, A. C., Yevich, R., and Logan, J. A.: Interannual and seasonal variability of biomass burning emissions constrained by satellite observations, Journal of Geophysical Research-Atmospheres, 108, 10.1029/2002jd002378, 2003.

Groemping, U.: Two simple estimators of relative importance in linear regression based on variance decomposition - Response, American Statistician, 61, 282-283, 2007.

Guenther, A., Karl, T., Harley, P., Wiedinmyer, C., Palmer, P. I., and Geron, C.: Estimates of global terrestrial isoprene emissions using MEGAN (Model of Emissions of Gases and Aerosols from Nature), ATMOS CHEM PHYS, 6, 3181-3210, 2006.

Hess, P., and Mahowald, N.: Interannual variability in hindcasts of atmospheric chemistry: the role of meteorology, ATMOS CHEM PHYS, 9, 5261-5280, 10.5194/acp-9-5261-2009, 2009.

Kruskal, W.: RELATIVE IMPORTANCE BY AVERAGING OVER ORDERINGS, American Statistician, 41, 6-10, 10.2307/2684310, 1987.

Lawrence, M. G., von Kuhlmann, R., Salzmann, M., and Rasch, P. J.: The balance of effects of deep convective mixing on tropospheric ozone, Geophysical Research Letters, 30, 10.1029/2003gl017644, 2003.

Olivier, J. G. J., Van Aardenne, J. A., Dentener, F. J., Pagliari, V., Ganzeveld, L. N., and Peters, J. A. H. W.: Recent trends in global greenhouse gas emissions: regional trends and spatial distribution of key sources, in: Non-CO2 Greenhouse Gases (NCGG-4), coordinator: van Amstel, A., Millpress, Rotterdam, ISBN 905966 043 9, 325–330,, 2005.

Strode, S. A., Rodriguez, J. M., Logan, J. A., Cooper, O. R., Witte, J. C., Lamsal, L. N., Damon, M., Van Aartsen, B., Steenrod, S. D., and Strahan, S. E.: Trends and variability in surface ozone over the United States, Journal of Geophysical Research-Atmospheres, 120, 9020-9042, 10.1002/2014jd022784, 2015.

van der Werf, G. R., Randerson, J. T., Giglio, L., Collatz, G. L., Mu, M., Kasibhatla, P. S., Morton, D. C., DeFries, R. S., Jin, Y., and T.T., v. L.: Global fire emissions and the contribution of deforestation, savanna, forest, agricultural, and peat fires (1997–2009), ATMOS CHEM PHYS, 10, 16153-16230, 2010.

Voulgarakis, A., Hadjinicolaou, P., and Pyle, J. A.: Increases in global tropospheric ozone following an El Nino event: examining stratospheric ozone variability as a potential driver, Atmospheric Science Letters, 12, 228-232, 10.1002/asl.318, 2011.

Young, P. J., Archibald, A. T., Bowman, K. W., Lamarque, J.-F., Naik, V., Stevenson, D. S., Tilmes, S., Voulgarakis, A., Wild, O., Bergmann, D., Cameron-Smith, P., Cionni, I., Collins, W. J., Dalsøren, S. B., Doherty, R. M., Eyring, V., Faluvegi, G., Horowitz, L. W., Josse, B., Lee, Y. H., MacKenzie, I. A., Nagashima, T., Plummer, D. A., Righi, M., Rumbold, S. T., Skeie, R. B., Shindell, D. T., Strode, S. A., Sudo, K., Szopa, S., and Zeng, G. (2013), Pre-industrial to end 21st century projections of tropospheric ozone from the Atmospheric Chemistry and Climate Model Intercomparison Project (ACCMIP), Atmos. Chem. Phys., 13, 2063-2090, doi:10.5194/acp-13-2063-2013.

Ziemke, J.R., A.R. Douglass, L.D. Oman, S.E. Strahan, and B.N. Duncan, "Tropospheric ozone variability in the tropics from ENSO to MJO and shorter timescales", Atmos. Chem. Phys. Discuss., 15, 6373-6401, doi:10.5194/acpd-15-6373-2015, 2015.

Causes of interannual variability over the southern hemispheric tropospheric ozone maximum

Junhua Liu[1,2], Jose M. Rodriguez[2], Stephen D. Steenrod[1,2], Anne R. Douglass[2], Jennifer A. Logan[3], Mark Olsen[2,4], Krzysztof Wargan[2,5], Jerald Ziemke[2,4]

[1] Universities Space Research Association (USRA), GESTAR, Columbia, MD, USA

[2] NASA Goddard Space Flight Center, Greenbelt, Maryland, USA

[3] School of Engineering and Applied Sciences, Harvard University, Cambridge, MA, USA

[4] Morgan State University, Baltimore, Maryland, USA

[5] Science Systems and Applications, Inc., Lanham, MD, USA

Correspondence to: Junhua Liu (junhua.liu@nasa.gov)

Junhua Liu 12/19/2016 11:27 AM

Deleted: Causes of interannual variability of tropospheric ozone over the Southern Ocean

Junhua Liu 2/2/2017 1:54 PM

Formatted: Font:(Default) Times, Font color: Black, Border:: (No border)

Abstract.

We examine the relative contribution of processes controlling the interannual variability (IAV) of tropospheric ozone over four sub-regions of the southern hemispheric tropospheric ozone maximum (SHTOM) over a twenty-year period. Our study is based on hindcast simulations from the National Aeronautics and Space Administration Global Modeling Initiative – Chemistry transport model (NASA GMI-CTM) of tropospheric and stratospheric chemistry, driven by assimilated Modern Era Retrospective-Analysis for Research and Applications (MERRA) meteorological fields. Our analysis shows that over SHTOM region, the IAV of the stratospheric contribution is the most important factor driving the IAV of upper tropospheric ozone (270 hPa), where ozone has a strong radiative effect. Over the south Atlantic region, the contribution from surface emissions to the IAV of ozone exceeds that from stratospheric input at and below 430 hPa. Over the south Indian Ocean, the IAV of stratospheric ozone makes the largest contribution to the IAV of ozone with little or no influence from surface emissions at 270 hPa and 430 hPa in austral winter. Over the tropical south Atlantic region, the contribution from IAV of stratospheric input dominates in austral winter at 270 hPa and drops to less than half but is still significant at 430 hPa. Emission contributions are not significant at these two levels. The IAV of lightning over this region also contributes to the IAV of ozone in September and December. Over the tropical southeastern Pacific, the contribution of the IAV of stratospheric input is significant at 270 hPa and 430 hPa in austral winter, and emissions have little influence.

Junhua Liu 12/19/2016 12:09 PM
Deleted: , even during September

1 Introduction

Tropospheric ozone plays a critical role in controlling the oxidative capacity of the troposphere through its photolysis in the presence of water vapor, generating hydroxyl radical (OH), the main atmospheric oxidant (e.g., Logan et al., 1981). It contributes to smog and is harmful to human and ecosystem health near the surface. It acts as a greenhouse gas especially in the upper troposphere (Lacis et al., 1990) and affects the radiative forcing of the climate system. Tropospheric ozone is produced by photochemical oxidation of CO and volatile organic compounds (VOCs) in the presence of nitrogen oxides (NO_X) (e.g., Logan et al., 1981). Downward transport of ozone from the stratosphere is also an important source of tropospheric ozone (e.g., Danielsen, 1968; Stohl et al., 2003). Deep convection and long-range transport of ozone and its precursors also modulate the tropospheric O_3 distributions (e.g., Chandra et al., 2009; Oman et al., 2011).

Our study is motivated by the presence of tropospheric ozone maximum over tropical and subtropical southern hemisphere as seen both in model simulations and GMAO assimilated ozone product derived from OMI/MLS satellite measurements (Figure 1). Although in the southern hemisphere tropospheric air is relatively "clean" and less polluted compared with the Northern Hemisphere, this tropospheric ozone column maximum reaches as high as 35DU and is comparable to the typical northern mid-latitude values of 30DU. The elevated tropospheric ozone column is centered over the south Atlantic from the equator to 30°S, and is part of the well-known tropical wave-one pattern first noted in observations made by the Nimbus 7 Total Ozone Mapping Spectrometer (TOMS) (e.g., Fishman et al., 1990; Ziemke et al., 1996). This ozone maximum extends westward to South America and the tropical southeastern Pacific, southeastward to southern Africa, south Indian Ocean along the latitude band of 30°S-45°S, and is a dominant global feature (Thompson et al., 2003; Sauvage et al., 2007). This elevated ozone region exists year-around, with a seasonal maximum in August - October, and a seasonal minimum in April - May.

This study provides an examination of the relative contributions of the factors that control the interannual variations of the southern hemisphere tropospheric ozone maximum over a twenty-year period. Prior studies have examined the processes that produce the southern hemisphere tropospheric ozone maximum (SHTOM), but consider only short periods or are limited in spatial scale. These studies concluded that horizontal and vertical transport of ozone precursors from regions of biomass burning (e.g., Jacob et al., 1996; Thompson et al., 1996; Pickering et al., 1996; Jenkins and Ryu, 2004b; Sauvage et al., 2006; Jourdain et al., 2007; Thouret et al., 2009), lightning NO_X (Martin et al., 2002; Jenkins and Ryu, 2004a; Kim et al., 2013; Tocquer et al., 2015) and stratospheric intrusions (Weller et al., 1996) all contribute to this tropospheric ozone column maximum. However, changes of the relative contributions of these factors to tropospheric ozone on inter-annual time scale over this region have not been examined in detail. Studies considering tropospheric ozone interannual variability have not focused on the SHTOM region. Hess and Mahowald (2009) used a CTM to quantify relative interannual variability in global model ozone in hindcast simulations with constant emissions and prescribed stratospheric ozone. The CTM was driven by two sets of meteorological fields: a) the National Center for Environmental Prediction/National Center for Atmospheric Research reanalysis; b) from a simulation using the Community Atmosphere Model (CAM-3) forced with observed sea surface temperatures. Their study found that relative IAV of ozone at 500 hPa shows the maximum between the Equator and 30S in June-July-August (JJA) and December-January-February (DJF). Zeng and Pyle (2005) used a climate/chemistry model to evaluate the ENSO effects on the interannual variability of tropospheric ozone. Their study concludes that STE variation induced by ENSO is one important factor driving the IAV of the global mean of tropospheric ozone. Voulgarakis et al. (2010) examined the drivers of interannual variability of the global tropospheric ozone using the p-TOMCAT tropospheric chemistry transport model (CTM). Their study shows that changing transport including the STE is important in determining the IAV of tropospheric ozone. Voulgarakis et al. (2011) demonstrated that increases in the amounts of stratospheric ozone entering the troposphere following El Niño events are mainly driven by changes in the STE. The influence of emissions is confined to areas of intense burning on the interannual timescale. Murray et al. (2013) examined the effects of lightning on the IAV in the tropical tropospheric ozone column based on the GEOS-Chem CTM with IAV in tropical lightning constrained by satellite observations from Lightning Imaging Sensors (LIS). Their study finds that lightning plays an important role in driving the IAV of tropical tropospheric ozone column, especially over East Africa, central Brazil, and in continental outflow in the eastern Pacific and the Atlantic, but their model does not reproduce the IAV in TCO except in East Africa and central Brazil. Liu et al. (2016) analyzed simulations from a global chemistry and transport model to show that the IAV in the stratospheric contribution significantly affects the IAV of upper tropospheric ozone at the SHADOZ station over Reunion (21°S). In this study, we focus on the SHTOM region and quantify the relative contributions of several factors to the tropospheric ozone interannual variability during the past twenty years. We examine the horizontal and vertical variations of these contributions by separating the SHTOM into four subregions and comparing their IAVs at two selected levels (270 hPa and 430 hPa). This analysis distinguishes between anthropogenic and natural sources on the IAV of the tropospheric ozone and their contributions to the radiative forcing changes.

In this study, we use a global chemistry transport model to identify the processes impacting observed interannual variability of the tropospheric ozone column maximum in southern hemisphere. We examine the model sensitivity of tropospheric ozone to different ozone sources through the use of multiple linear regression. We include stratospheric input and emissions as two major predictor variables in our regression. We include the lightning NO_X as the third factor in our regression model over the tropical south Atlantic region, where ozone is sensitive to the IAV of lightning NO_X as found in Murray et al (2013). In our multiple linear regression, a regression coefficient that is significantly different from zero at the 95% confidence level implies that the corresponding process contributes significantly to the variation of simulated ozone. To estimate the variance explained by each predictor, we first calculate the sequential sums of squares over ordering of predictors (see supplementary materials). The sequential of squares depends on the predictors already in the model; we therefore do the calculation for every possible order in which predictors can enter the model. We then average all the sequential sums of squares to yield an adjusted sum of squares (Kruskal, 1987; Chevan and Sutherland, 1991; Groemping, 2007). This method accounts for the likely possibility that the two predictors are not orthogonal. We use the adjusted sum of squares to quantify the relative contributions of each predictor to the interannual variability of tropospheric ozone. Our study focuses on austral winter season when the subtropical jet related stratosphere - troposphere exchange reaches the seasonal maximum (Karoly et al., 1998; Bals-Elsholz et al., 2001; Nakamura and Shimpo, 2004). Southern hemisphere biomass burning (e.g., Liu et al., 2010; 2013) also reaches the maximum during this season.

Section 2 briefly describes the model and simulations, including the standard chemistry simulation, the stratospheric O_3 tracer simulation, and the tagged CO simulation. It also describes GEOS-5 ozone assimilation, as the assimilated fields are used to evaluate model performance over the southern hemisphere extra-tropics and tropics as discussed in the first part of Section 3. The second part of Section 3 presents a diagnostic study of controlling factors, including stratosphere input, surface emissions and lightning, on the tropospheric ozone IAV relying on a series of hindcast simulations from 1992 to 2011. Section 4 is a summary and conclusion.

2 Model and Data

2.1 Model

We used the Global Modeling Initiative chemical transport model (GMI-CTM) (Duncan et al., 2007; Strahan et al., 2007), driven by MERRA reanalysis meteorology (Rienecker et al., 2011, http://gmao.gsfc.nasa.gov/research/merra/). The native resolution of the MERRA field is 0.67° × 0.5° with 72 vertical levels; we regrid it to 2°x2.5° horizontal grid for input to the GMI-CTM simulations in this study.

The chemical mechanism used in GMI-CTM represents stratospheric and tropospheric chemistry with offline aerosols input from GOCART model simulations (Chin et al., 2002). The GMI-CTM hindcast simulation has been used and compared to observations in many recent studies. Strahan et al. (2013) showed excellent agreement between simulated and MLS ozone profiles in the Arctic lower stratosphere. Liu et al. (2016) shows the GMI-CTM hindcast and ozonesonde agree very well on the annual cycles and IAV over Reunion from lower troposphere to the upper troposphere. Strode et al. (2015) shows that the GMI-CTM hindcast reproduces the seasonal cycle and IAV of observed surface ozone over United States from Environmental Protection Agency (EPA)'s Clean Air Status and Trends Network (CASTNET).

The GMI-CTM standard simulation (labeled as Hindcast-VE) used in this study for 1992-2011 includes monthly and inter-annually varying emissions with anthropogenic, biomass burning, and biogenic sources. Anthropogenic emissions are based on the EDGAR 3.2 Inventory (Olivier et al., 2005), overwritten with available regional inventories for North America, Europe, Asia and Mexico. More details are given in Strode et al. (2015). Biomass burning emissions are from the Global Fire Emission Database, GFED3 (van der Werf et al., 2010). Emission before 1997 are obtained from GFED3 emission climatology averaged for 2001 to 2009 applied with regional-scale IAV, which was derived from satellite information on fire activity (ATSR) and/or aerosol optical depths from the Total Ozone Mapping Spectrometer (TOMS) by Duncan et al. (2003). Biogenic emissions of isoprene and monoterpenes follow the latest version of the MEGAN algorithm (Guenther et al., 2006). Besides the standard simulation, we carry out a control run for 1991-2011 by repeating the anthropogenic and biomass emissions for 2000. The comparison between the control and standard simulation removes the possible impact of IAV in meteorology and allows us to quantify effects of emission IAV on ozone IAV.

In our GMI-CTM, the lightning parameterization follows the scheme described by Allen et al (2010). The regional lightning NO_X emission, calculated online by coupling to the deep convective transport in the model, varies from year to year. The global total of NO_X from lightning is fixed at 5.0 TgN/yr.

Junhua Liu 12/19/2016 3:31 PM
Deleted: The sources of emissions in the GMI-CTM standard simulation are summarized in the recent study of Strode et al. (2015). Besides the standard simulation, we also carry out a control run with constant emissions fixed at the year 2000 levels to quantify effects of emission IAV on ozone IAV. ... [1]

Methane mixing ratios are specified in the two lowest model levels, using time dependent zonal means from National Oceanic and Atmospheric Administration / Global Monitoring Division (NOAA/GMD). Other long-lived source gases important in the stratosphere, such as N_2O, CFCs, halocarbons are prescribed at the two lowest model levels following the A2 scenario by (WMO, 2014). Stratospheric aerosol distributions/trends are from International Global Atmospheric Chemistry/Stratospheric Processes And their Role in Climate (IGAC/SPARC) and have IAV (Eyring et al., 2013).

The model includes a stratospheric O_3 tracer ($StratO_3$). The $StratO_3$ is defined relative to a dynamically varying tropopause tracer (e90) (Prather et al., 2011). The e90 tracer is set to a uniform mixing ratio (100 ppb) at the surface with 90 days e-folding lifetime. In our simulation, the e90 tropopause value is 75 ppb. The $StratO_3$ tracer is set equal to O_3 in the stratosphere and is removed in the troposphere with the same loss frequency (chemistry and deposition) archived from daily output of the standard chemistry model simulation with yearly-varied emission in this study. Using the $StratO_3$ tracer allows quantification of O_3 of stratospheric origin in the troposphere at a given location and time. This approach has also been adopted in the high resolution GFDL AM3 model (Lin et al., 2012).

Junhua Liu 12/20/2016 2:40 PM
Deleted: This artificial tracer

In this study, we also conducted a tagged CO simulation to examine the emission sources during the same period as the full chemistry simulation. The tagged CO simulation has horizontal resolution of 1°x1.25°. The primary chemical loss of CO is through reactions with OH radicals, which are archived from the respective standard chemistry simulation with yearly-varied emissions. The chemical production and loss rates of CO in the stratosphere were archived from the respective standard chemistry simulations.

2.2 GMAO GEOS-5 Ozone Assimilation

We used assimilated tropospheric ozone to evaluate model performance. This assimilated dataset is produced by ingesting OMI v8.5 total column ozone and MLS v3.3 ozone profiles into a version of the Goddard Earth Observing System, Version 5 (GEOS-5) data assimilation system (Rienecker et al., 2011). No ozonesonde data are used in the assimilation. Wargan et al. (2015) provides details of the GEOS-5.7.2 assimilation system, which for this application is produced with 2° x 2.5° horizontal resolution and with 72 vertical layers between the surface and 0.01 hPa. For the troposphere, the assimilation only applies a dry deposition mechanism at the surface without any chemical production or loss. This algorithm works since the ozone lifetime is much longer than the six-hour analysis time on which the background field is corrected by observations. Ziemke et al. (2014) evaluated the tropospheric ozone profiles derived from three strategies based on OMI and MLS measurements, including this GEOS-5 assimilation, trajectory mapping and direct profile retrieval using residual method, with ozonesonde observations and GMI model simulations. They show that the ozone product (500 hPa to tropopause) from the GEOS-5 assimilation is the most realistic. Wargan et al. (2015) also demonstrate that the ozone between 500 hPa and the tropopause from GEOS-5 assimilation is in good agreement with independent observations from ozonesondes. The assimilation applies the OMI averaging kernels in the troposphere, but the weight of OMI kernels decreases sharply below 500 hPa (Personal communication with K. Wargan). Considering that in the lower troposphere there is no direct observational constraint in the analysis, we use ozone mixing ratio at 270 hPa and 430 hPa as well as partial column ozone integrated from 500 hPa to the tropopause from GEOS-5 assimilation as a reference value to evaluate our GMI model simulation. To compare the GEOS-5 assimilated tropospheric partial column above 500 hPa with GMI-CTM ozone simulation, we use the same tropopause as defined by the lower of the 3.5 potential vorticity units (PVU) isosurface and the 380 K isentropic surface.

3 Results

3.1 Temporal and spatial distribution of SHTOM in GMI-CTM and GMAO GEOS-5 assimilated ozone product

Figure 1 shows the spatial pattern of southern hemispheric partial column ozone (from 500 hPa to the tropopause) in four seasons averaged over 2005 to 2011 from the GMAO GEOS-5 assimilated dataset and the GMI-CTM hindcast simulations. To account for a low bias in the GEOS-5 ozone product (Wargan et al., 2015), we added 2.5 DU to the assimilated column in the tropics (0-30°S). The GMI-CTM simulation reproduces the seasonality and spatial distribution of southern hemispheric ozone maximum as shown in GEOS-5 assimilated product with a) the elevated ozone centered over the Atlantic Ocean from the equator to 40°S; b) the ozone maximum extending southeastward to southern Africa and the Indian Ocean in the latitude band of 30°S-45°S; c) the relatively weaker enhancement extending westward to South America and the tropical southeastern Pacific. The ozone maximum is strongest in austral winter-spring and weakest in austral fall. Both GMI-CTM and GEOS-5 assimilation show the very low tropospheric ozone over the western Pacific and the tropical eastern Indian Ocean, where the ozone - poor marine boundary layer air is lifted into the upper troposphere (Folkins et al., 2002; Solomon et al., 2005).

3.2 Subregions of SHTOM

The tropospheric ozone distribution in any region depends on the advection and mixing, its proximity to the polluted area, and descent of ozone-rich air from the stratosphere. We show in Figure 2 the maps of simulated O_3 and $StratO_3/O_3$ at 430 hPa averaged over 1992 to 2011 in September, when the southern hemisphere biomass burning peaks. The $StratO_3/O_3$ ratio represents the fraction of tropospheric ozone from the stratosphere and is used to identify the regions with distinct stratospheric input. Differences in the spatial patterns of the maximum/minimum in ozone mixing ratio and $StratO_3/O_3$ ratio identifies regions where ozone is affected by factors other than the stratospheric input.

The region with minimum stratospheric ozone contribution occurs along the equator. In the tropics, the southward extension of regions with minimum stratospheric ozone contribution shows zonal variation, reaching 5°S to 10°S over tropical eastern Pacific and tropical Atlantic, and further south to approximately 15°S over the Indian Ocean and the Maritime Continents, which is closely related to the Walker Circulation. In this tropical zonal circulation air rises over the Maritime Continents (together with deep convection) and descends over the eastern Pacific (Bjerknes, 1969). Similar zonal circulation is found over the Atlantic with rising due to radiative heating over tropical Africa and South America and sinking due to radiative cooling over the tropical Atlantic (Julian and Chervin, 1978). The longitudinal variation of ozone at 430 hPa in the tropics is in agreement with the changes of $StratO_3/O_3$, showing ozone minimum over Maritime Continents as well as elevated ozone over eastern Pacific and Atlantic. Within the Atlantic, despite the smaller stratospheric contribution, the tropics have higher ozone mixing ratio (>80 ppb) than the subtropics at 430 hPa, and other sources must also contribute to the ozone maximum over tropical south Atlantic. Ozone over the tropical southeastern Pacific is also slightly elevated. The maximum stratospheric influence is found over the southern Indian and Pacific Oceans centered on 30°S, co-located with the tropospheric O_3 maximum over these regions. Both ozone and $StratO_3/O_3$ over the subtropics show strong longitudinal variations, with the co-located maxima over the south Indian Ocean. The ozone minimum at 430 hPa at 30°S occurs over the eastern Pacific region, while the minimum contribution of the stratospheric input is over the south Atlantic region. Given the spatial variations of the maximum/minimum in $StratO_3/O_3$ ratio and ozone mixing ratio, we separate the southern hemispheric ozone maximum into four sub-regions: 1) Tropical southeastern Pacific (0-20°S, 150°W-60°W); 2) Tropical South Atlantic (0-15°S, 60°W-40°E); 3) Subtropical South Atlantic (15°S-45°S, 60°W-40°E); 4) Subtropical South Indian Ocean (15°S-45°S, 40°E-150°E). We show in Figure 3 the maps of the IAV of simulated O_3 at 270 hPa and 430 hPa. The IAV is represented by the standard deviation of ozone anomalies (removing the monthly mean averaged from 1992 to 2011) over 1992-2011. Relatively stronger ozone IAV happens

Junhua Liu 12/31/2016 6:00 AM
Deleted: It extends southward to approximately 10°S over South America and further south to approximately 15°S over the Indian Ocean and the Maritime Continents.

Junhua Liu 12/31/2016 5:56 AM
Deleted: strong

Junhua Liu 12/20/2016 3:20 PM
Deleted: meridional

Junhua Liu 12/31/2016 6:00 AM
Deleted: that

Junhua Liu 12/20/2016 3:21 PM
Deleted: meridional

Junhua Liu 12/20/2016 3:21 PM
Deleted: meridional

Junhua Liu 12/31/2016 6:03 AM
Deleted: South America, tropical Africa and

Junhua Liu 12/31/2016 9:26 AM
Deleted: of

Junhua Liu 12/31/2016 6:49 AM
Deleted: Southern Ocean

over subtropical south Atlantic and subtropical south Indian Ocean at 270 hPa. At 430 hPa, Tropical southeastern Pacific and tropical South Atlantic has slightly larger IAV. In this paper, we examine and quantify the relative roles of dynamics and chemistry on the IAV of tropospheric ozone variations over these selected regions during the past twenty years.

Figure 4 compares the anomalies of modeled and assimilated upper tropospheric ozone columns (UTOC, integrated from 500 hPa to the tropopause) as well as the anomalies of corresponding tropospheric ozone mixing ratio at 270 hPa and 430 hPa over two tropical sub-regions (tropical south Atlantic and tropical southeastern Pacific) from 2005 to 2011. The anomalies are calculated by removing the monthly mean averaged from 2005 to 2011. The short time scale variations in the model simulation tend to be greater compared to that in the assimilated ozone products, especially over the tropical south Atlantic region. But in general, the GMI-CTM hindcast simulation captures the assimilated IAV of the tropospheric ozone at these two levels as well as for the UTOC. Over the tropical south Atlantic, the modeled IAV agrees with the phase changes of assimilated ozone IAV but the simulation overestimates the assimilated ozone maximum in 2010 and underestimates the assimilated minima in 2007 and 2011 at both levels. Over the tropical southeastern Pacific, the IAV is influenced by ENSO related changes in dynamics (e.g., Ziemke et al., 2010;2011; Oman et al., 2013). The simulation reproduces much of the assimilated IAV, showing high ozone anomalies after 2005, 2010 La Nina year and negative ozone anomalies after strong El Niño year in 2009. However, during October 2006 to January 2007, the simulation shows a pronounced ozone peak, especially at 270 hPa, which is not seen in the assimilated ozone. Logan et al. (2008) examined interannual variations of tropospheric ozone profiles in October-December between 2005 and 2006 based on the satellite observations from Tropospheric Emission Spectrometer (TES). The TES data agree with what we found in the GMI-CTM model simulation, showing ozone enhancement over the tropical southeastern Pacific (150°W-60°W, 0-12°S) region in November 2006 relative to 2005 (~5-10 ppb at 250 hPa and 0-5 ppb at 400 hPa, Figure 3 of Logan et al., 2008). The agreement between TES and GMI-CTM indicates a possible low bias of GMAO assimilated ozone during late 2006, as a result of the low sensitivity

Junhua Liu 1/15/2017 2:49 PM
Deleted: W

Junhua Liu 1/15/2017 2:49 PM
Deleted: 3

Junhua Liu 1/10/2017 3:06 PM
Deleted: modeled and assimilated tropospheric

Junhua Liu 1/10/2017 3:06 PM
Deleted: as well as the anomalies of corresponding upper tropospheric ozone columns (UTOC, integrated from 500 hPa to the tropopause)

of OMI (Wargan et al., 2015).

Figure 5 shows the similar comparison as Figure 4, but over the two subtropical regions. Over the South Atlantic region, the assimilated ozone has similar but stronger IAV than that over the tropical southeastern Pacific region, showing the largest ozone year-by-year variation (~20ppb at 270 hPa) from October 2009 to October 2010, and the GMI-CTM simulation reproduces this variation quite well. Over the South Indian region, our model reproduces most of the variations in magnitude and phase, but shows anti-phase variations in late 2006/early 2007, which substantially affected the calculated correlation coefficients between model and assimilated ozone. The simulated upper tropospheric ozone column reproduces well the IAV in the assimilated ozone column except for the late 2006. In general, agreement between the simulated and assimilated results confirms the suitability of the model for investigations of the controlling factors on the tropospheric ozone IAV over these regions.

The left column of Figure 6 presents the monthly profiles of correlation coefficients between the simulated ozone and $StratO_3$ over the four sub-regions. Strong positive correlations between $StratO_3$ and O_3 are observed in most seasons in the upper troposphere even over two tropical regions. Stratospheric influence plays a big role during austral winter-spring and reaches its seasonal maximum in August, when the subtropical jet system is strongest and moves to its northern-most location. Over the two subtropical regions, the strong stratospheric influence persists throughout the whole troposphere (r > 0.8 at 700 hPa) in August. Over tropical south Atlantic region, the strong stratospheric influence is limited to the upper troposphere in austral winter-spring and decreases sharply with decreasing altitude. Over the tropical southeastern Pacific, the strong stratospheric influence persists year-long at the upper troposphere and reaches as low as ~400 hPa except for December.

The right column of Figure 6 shows the seasonal profiles of correlation coefficients between ozone and ozone from emissions ($EmissO_3$). The $EmissO_3$ is the difference between the simulations with varied and constant emission. Over the two subtropical regions, there are two seasonal maxima in the correlations between ozone and $EmissO_3$. The first occurs in September at the lower troposphere and decreases with increasing altitude, the second is in December/January showing opposite vertical gradient with

Junhua Liu 1/15/2017 2:50 PM
Deleted: 4

Junhua Liu 1/15/2017 2:50 PM
Deleted: 3

Junhua Liu 1/15/2017 3:01 PM
Deleted: the assimilated ozone has weaker IAV than over other regions. O

Junhua Liu 1/15/2017 2:50 PM
Deleted: 5

Junhua Liu 1/15/2017 2:50 PM
Deleted: 5

stronger correlations in the upper and middle troposphere. Over the tropical southeastern Pacific region, the influence from emissions shows a similar double-peak pattern, but with the first maximum localized at the surface and the second peak localized in the upper troposphere. Over the tropical south Atlantic, the influence of emissions is very small. South America and southern Africa are two major nearby burning regions. Emissions over South America have much larger IAV than those over southern Africa, although African emissions are larger in absolute terms (Sauvage et al., 2007; Liu et al., 2010; Voulgarakis et al., 2015). Sauvage et al (2007) argued that emissions over South and Southeast Asia could be transported southward in the upper troposphere through the Tropical Easterly Jet and affect ozone over Africa, the Atlantic and Indian Ocean (Hoskins and Rodwell, 1995; Rodwell and Hoskins, 2001). Meanwhile, emissions over this region also show large IAV (Voulgarakis et al., 2015). Therefore, the interannual emission changes in South America (0-20°S, 72.5°W-37.5°W), southern Africa (5°S-20°S, 12°E-38°E) and South and Southeast Asia (70°E-125°E, 10°S-40°N) may all affect the IAV of ozone due to emission changes in the southern hemisphere. In this study, we rely on tagged CO simulation to quantify the influence of biomass burning emissions from these three burning regions during months when emission IAV contributes significantly to the IAV of ozone.

In the next section, we choose August (the seasonal maximum of stratospheric input into the lower troposphere), September and December (the seasonal maximum of emission contribution) as three example months to examine the relative roles of different factors on IAV of tropospheric ozone over these regions.

3.3 Factors controlling IAV in ozone in the middle and upper troposphere

3.3.1 South Atlantic Region

Figure 7 shows the multiple regression results over the South Atlantic region. It compares the simulated ozone anomalies to that calculated from two regression variables: $StratO_3$ and $EmissO_3$ at 270 hPa and 430 hPa in August, September and December. The fitted ozone anomalies in generally reproduce the IAV obtained from the GMI-CTM simulation. The explained proportion of variability in simulated ozone anomalies by

Junhua Liu 12/31/2016 7:56 AM
Deleted: the

Junhua Liu 12/31/2016 7:56 AM
Deleted: eastern regions (India, South-East Asia, Australia)

Junhua Liu 12/31/2016 7:57 AM
Deleted: the eastern region

Junhua Liu 12/31/2016 7:57 AM
Deleted: the eastern region

Junhua Liu 1/15/2017 2:50 PM
Deleted: 6

$StratO_3$ and $EmissO_3$ is mostly above 50% and reaches as high as ~ 76% in December, at 270 hPa, which demonstrates that $StratO_3$ and $EmissO_3$ are sufficient to explain the IAV of tropospheric ozone over the south Atlantic region. In August at 430 hPa, the fitted ozone anomalies have a slightly weaker correlation with the simulated ozone and show less IAV compared to the ozone anomalies in GMI-CTM.

Figure 8 exhibits regression results in a way that highlights the relative contributions of the IAV of stratospheric input and emission on the IAV of ozone over South Atlantic. The three panels represent results from August, September and December from 1992 to 2011. Each panel has two columns, which illustrate the respective contribution from changes in $StratO_3$ and $EmissO_3$ on the IAV of ozone mixing ratio. The left column of each panel compares the anomalies of $StratO_3$ (blue) and simulated ozone mixing ratio (black) from the GMI-CTM model at 270 and 430 hPa. The right column compares the simulated O_3 residual after removing the regression from $StratO_3$ (black line) and $EmissO_3$ (green line) at these two levels. The regression coefficient (β) and its 95% confidence level are labeled in each panel and help us to determine whether the corresponding contribution is significant to explain the variation of simulated ozone. As discussed before, $EmissO_3$ reflects the effects from surface emission changes on ozone variations at interannual time scale. The stratospheric input reaches its seasonal maximum in August, during which the stratospheric contribution is significant throughout the troposphere, explaining about 66% of the simulated ozone variance at 270 hPa and 37% at 430 hPa. The contributions from emission changes are very small and insignificant at these two levels in August. In September, the IAV of stratospheric input explains about 55% of the IAV in ozone at 270 hPa. The contribution decreases but is still significant at 430 hPa. The IAV of surface emissions contributes substantially to the IAV of ozone in September. The influence of emissions exceeds that of the stratosphere and explains about 35% of IAV in ozone at 430hPa. In December, the contribution from stratospheric input to the IAV of ozone is dominant (~47%) at 270 hPa. The contribution from emission is also significant at this level and explains 28% variance of IAV of ozone. At 430 hPa, the contribution from emission exceeds that from stratospheric input.

We quantify emission contributions from three burning regions using a tagged CO simulation. Figure 9 shows standardized anomalies of the tagged CO tracers over South

Junhua Liu 1/15/2017 2:50 PM
Deleted: 7

Junhua Liu 1/15/2017 4:38 PM
Deleted: 41

Junhua Liu 1/15/2017 4:39 PM
Deleted: 3

Junhua Liu 1/14/2017 2:18 PM
Deleted: 50

Junhua Liu 1/15/2017 4:50 PM
Deleted: s

Junhua Liu 1/15/2017 4:50 PM
Deleted: are

Junhua Liu 1/15/2017 4:39 PM
Deleted: 60

Junhua Liu 1/15/2017 4:52 PM
Deleted: but insignificant at 430 hPa

Junhua Liu 1/15/2017 4:49 PM
Deleted: Emission influence is significant at both levels.

Junhua Liu 1/15/2017 4:47 PM
Deleted: However, unlike that of September, the influence of emissions on IAV of tropospheric ozone is great at 270 hPa (~40%) than at 430 hPa (~36%).

Junhua Liu 1/15/2017 2:50 PM
Deleted: 8

Atlantic from three burning source regions, including southern Africa (red), South America (blue) and South and Southeast Asia (green) and their comparison with the $EmissO_3$ at 270 and 430 hPa in September and December from 1992 to 2011. The direct downwind transport of emissions from South America contributes most to the ozone variability from emissions over this region in September at both levels and the effects are most significant in the lower level (~58% at 430 hPa). In the upper troposphere, besides the contribution from S. America, the uplift and cross-equator transport of pollutants from South and Southeast Asia also contributes (>10%) to the ozone variation over South Atlantic region. The contribution from southern Africa is small and less than 10% at both levels. We also note that both $StratO_3$ and $EmissO_3$ show a minimum in 2009 and a maximum in 2010. There was a strong El Niño event in the year 2009/2010. Neu et al. (2014) identified the increased stratospheric circulation in 2010 driven by El Niño/easterly QBO based on TES data. A few other studies (e.g., Chen et al., 2011; Lewis et al., 2011) found that combined effects of 2009/2010 El Niño and warmer than normal Atlantic SST produced a severe drought over S. America and caused extensive biomass burning emission in 2010 dry season. Therefore, the agreements between changes in the $StratO_3$ and $EmissO_3$ over 2009/2010 are at least partly driven by ENSO. Similar tropospheric ozone anomalies are observed after 1997 and 2006 El Niño event. Olsen et al. (2016) examined the magnitude and spatial distribution of ENSO effects on tropospheric column ozone using the assimilated fields and found a statistically significant negative response of tropospheric column ozone to the Niño 3.4 index over South Atlantic Ocean.

Junhua Liu 12/31/2016 7:58 AM
Deleted: eastern region

Junhua Liu 12/31/2016 7:58 AM
Deleted: eastern region

Junhua Liu 12/31/2016 8:10 AM
Deleted: ENSO

In December, emissions from South America and southern Africa do not contribute substantially to the IAV of $EmissO_3$. Emissions from South and Southeast Asia dominate, explaining 83% and 77% variance of $EmissO_3$ IAV at 270 hPa and 430 hPa. The pollutants from South and Southeast Asia have the stronger influence at the upper troposphere because of their transport pathway as discussed in Sauvage et al. (2007). Therefore, the emission contribution of tropospheric ozone IAV becomes significant at 270 hPa in December.

Junhua Liu 12/31/2016 7:58 AM
Deleted: eastern region

In summary, over the South Atlantic region, the stratospheric input plays a dominant role in the upper troposphere with a seasonal maximum in August. At 430 hPa the contribution from emission changes to the IAV of ozone exceeds that of stratospheric input in September and December. A tagged CO simulation from 1992 to 2011 shows the direct downwind transport of pollutants from South America is the largest contributor to $EmissO_3$ in September, and it is strongest near the surface. In December, cross-equator transport of South and Southeast Asia pollutants is the most important source of IAV due to emissions, and the effects are stronger in the upper troposphere.

3.3.2 South Indian Ocean

Over the south Indian Ocean, the fitted and simulated ozone anomalies are in excellent agreement (Figure 10). The explained proportion of variability in simulated ozone anomalies by $StratO_3$ and $EmissO_3$ is as high as ~ 88% in August at 270 hPa. We show relative contribution to the IAV in ozone due to stratospheric input and emission as obtained from multiple linear regression in Figure 11. In August and September, stratospheric input contributes more than 85% to ozone IAV at 270 hPa. The stratospheric contribution decreases slightly but is still dominant and significant at 430 hPa (~49% in August and 60% in September). The emission contribution, which is mainly from downwind transport of pollutants from S. America and southern Africa (Figure 12), is most important at 430 hPa in September but accounts for only 13% of ozone IAV. The emission contribution is smaller in August. In December, both stratospheric input and surface emission influence the IAV of ozone. The contribution from stratospheric input exceeds that from emissions at 270 hPa and becomes slightly weaker at 430 hPa. Examining the tagged sources simulation shows that emissions from South and Southeastern Asia regions are the largest source of ozone IAV at 270 hPa and 430 hPa in December with a stronger influence at the upper troposphere (Figure 12). These results show that stratospheric ozone makes a significant contribution to the tropospheric ozone variability over the South Indian Ocean, with the largest influence in the upper troposphere in austral winter. Emission influence from nearby pollution in the boundary layer is relatively weak and only significant in September, one month after the southern hemisphere peak-burning season. In the upper troposphere, the cross-equator transport of pollutants from South and Southeast Asia is the major emission source

Junhua Liu 1/15/2017 2:50 PM
Deleted: 9

Junhua Liu 1/15/2017 2:50 PM
Deleted: 0

Junhua Liu 1/15/2017 4:55 PM
Deleted: 50

Junhua Liu 1/15/2017 4:55 PM
Deleted: 64

Junhua Liu 1/15/2017 2:51 PM
Deleted: 1

Junhua Liu 1/15/2017 4:56 PM
Deleted: 27

Junhua Liu 1/10/2017 3:53 PM
Deleted: eastern

Junhua Liu 1/15/2017 2:51 PM
Deleted: 1

affecting the ozone variability. The influence peaks in December in the upper troposphere and extends to the middle troposphere.

3.3.3 Tropical South Atlantic

In the upper troposphere, lightning produces nitrogen oxides (NO_X) and promotes the photochemical ozone production (e.g., Pickering et al., 1993). Murray et al. (2013) shows that the IAV of tropical tropospheric ozone column is sensitive to the IAV of lightning over the tropical south Atlantic region. We therefore add the lightning NO_X as the third variable besides $StratO_3$ and $EmissO_3$. We test whether the addition of lightning NO_X improves the regression model significantly. Figure 13 shows the comparison between simulated and fitted ozone anomalies without and with lightning NO_X. During the "dry season" months of August and September, when the subtropical jet related STE (Karoly et al., 1998;Bals-Elsholz et al., 2001;Nakamura and Shimpo, 2004) reaches a seasonal maximum, the lightning activity reaches a seasonal minimum over the southern hemisphere. The fitted ozone anomalies based solely on $StratO_3$ and $EmissO_3$ (red) show high correlations (r = 0.8 in August, r = 0.74 in September) with that simulated from GMI-CTM at 270 hPa. Agreement between simulated and fitted ozone does not change in August and improves slightly in September by adding lightning NO_X in regression. In September, the simulated ozone anomaly shows a minimum (~ -6 ppb) in 2007 and a peak (~ 5ppb) in 2010 at 430 hPa, but the IAV from 2007 to 2010 is almost missing in the fitted ozone anomaly, which indicates that other factors drive the IAV of ozone over tropical south Atlantic during this period. During the "wet season" month of December, the lightning activity reaches its seasonal maximum. Our regression based on $StratO_3$ and $EmissO_3$ does not capture well the IAV of GMI-CTM simulated ozone at either level. The fitted ozone reproduces many of the IAV of simulated ozone after including lightning NO_X in the regression, indicating a strong influence from the lightning NO_X in December.

Figure 14 shows the regression results of relative contributions of stratospheric input and surface emission on the IAV of ozone. As discussed above, the tropical south Atlantic is in the descending branch of the Walker Circulation. Therefore, even though this region is located in the tropics, the IAV of stratospheric input still plays a dominant role and

Junhua Liu 1/15/2017 2:51 PM
Deleted: 2

Junhua Liu 12/31/2016 8:21 AM
Deleted: ies

Junhua Liu 1/15/2017 2:51 PM
Deleted: 3

explains 60% in August and 51% in September of ozone variance in the upper troposphere. The stratospheric contribution, associated with radiative descent over this region, drops to less than 38% in August and 18% in September at 430 hPa but is still significant during these two months. Emission influences are not significant at either level in September. Examination of the simulation shows that emission contribution is limited even at lower levels; the emission contribution becomes significant and explains ~30% variance of ozone at ~700 hPa (not shown). In December, neither stratospheric input nor emission contributes much to the IAV of ozone.

In the model, the lightning emissions take place in connection with deep convective events (Allen et al., 2010). Increase in deep convection produces more upper tropospheric NO_X from lightning, which results in more ozone production. On the other hand, deep convection affects the upper tropospheric ozone budget through its direct transport of surface air. In December, biomass burning in the Southern Hemisphere is at its seasonal minimum. Air over tropical south Atlantic is relatively clean with low CO (Liu et al., 2010). Deep convection over a clean region reduces upper tropospheric ozone by mixing up ozone-poor air from near the surface. This effect could be opposite if deep convection happens over a polluted region with relatively high ozone and its precursors (Lawrence et al., 2003; Ziemke, et al., 2015). Use of the correlation to identify influence from the lightning NO_X does not separate the two outcomes of IAV in convection, thus the sign of the correlation between variations in lightning NO_X and upper tropospheric ozone can be positive or negative. The correlation is positive if the contribution from lightning NO_X exceeds the contribution from convective transport or if transport of polluted air increases ozone. The correlation is negative if transport of clean air overwhelms ozone production from lightning NO_X. Figure 15 compares the model residual after removing the contributions from $StratO_3$ and $EmissO_3$ with the lightning NO_X at 270 hPa in September and December. In September the IAV of lightning plays a minor but significant role in the IAV of ozone in the upper troposphere. In December, the changes in lightning NO_X have a significant impact on the ozone IAV, but show a negative regression (β_3=-1.29), which indicates that the transport and mixing of clean surface air exceeds ozone production from lightning NO_X emissions with a net negative impact of IAV in convection.

Junhua Liu 1/15/2017 4:58 PM
Deleted: 64

Junhua Liu 1/15/2017 4:59 PM
Deleted: 50

Junhua Liu 1/15/2017 4:59 PM
Deleted: 30

Junhua Liu 1/15/2017 4:59 PM
Deleted: at 430 hPa

Junhua Liu 12/31/2016 8:30 AM
Deleted: due to mixing.

Junhua Liu 12/31/2016 8:30 AM
Deleted: positive

Junhua Liu 1/15/2017 2:51 PM
Deleted: 4

Junhua Liu 1/15/2017 5:03 PM
Deleted:

Junhua Liu 2/2/2017 1:54 PM
Formatted: Subscript

Junhua Liu 1/15/2017 5:01 PM
Deleted: correlation

3.3.4 Tropical southeastern Pacific

Figure 16, 17 and 18 show the similar comparisons but over the tropical southeastern Pacific region. The fitted ozone anomalies show moderate but still significant correlations with that simulated from GMI-CTM in August and September. In December, the fitted ozone IAV agrees very well with the GMI-CTM simulated ozone IAV at 270 hPa. At 430 hPa the agreement collapses and the fitted ozone does not show strong IAV as seen in the GMI-CTM simulated ozone (Figure 16). Figure 17 shows that IAV in stratospheric input significantly affects the ozone IAV during these three months, explaining 28-40% of the variance of simulated ozone at 270 hPa. Emissions contribution is quite small in August and September, but is significant and explains 17% of simulated ozone IAV in December at 270 hPa. The tagged CO simulations show that the tropical southeastern Pacific region is influenced by nearby pollutants from South America, and also by the cross-equator transport of pollutants from South and Southeast Asia (Figure 18). Previous studies (e.g., Chandra et al., 1998; Sudo and Takahashi, 2001; Chandra et al., 2002; Ziemke and Chandra, 2003; Doherty et al., 2006; Chandra et al., 2009; Oman et al., 2011) show that ENSO has its strongest impact in the tropical Pacific basin. In August, the ITCZ is located at its northernmost location north of the Equator. Radiative sinking motion still dominates over the tropical southeastern Pacific in the middle - upper troposphere (Liu et al., 2010). Therefore, the emissions contribution from South America is quite small at 430 hPa and 270 hPa as shown in Figure 17. During an El Niño year, warmer SST with increased convection and large-scale upwelling begin in August, inhibiting the radiative sinking motion and resulting in ozone decrease in the middle-upper troposphere over this region. Our comparison shows strong negative correlation in August between IAV of middle-upper tropospheric ozone anomalies over this region and Niño 3.4 index during the past twenty years (Figure 19).

4 Summary and Discussion

Both model simulations and GEOS-5 assimilated ozone product derived from OMI/MLS show a tropospheric ozone column maximum centered over the south Atlantic from the equator to 30°S. This ozone maximum extends westward to South America and the

Junhua Liu 2/2/2017 1:54 PM
Formatted: Font:Font color: Black

Junhua Liu 1/15/2017 2:51 PM
Deleted: 5

Junhua Liu 1/15/2017 2:51 PM
Deleted: 6

Junhua Liu 1/15/2017 2:51 PM
Deleted: 7

Junhua Liu 1/15/2017 2:51 PM
Deleted: 5

Junhua Liu 1/15/2017 2:52 PM
Deleted: 6

Junhua Liu 1/15/2017 5:04 PM
Deleted: 25-38%

Junhua Liu 1/15/2017 5:04 PM
Deleted: 28

Junhua Liu 12/31/2016 7:57 AM
Deleted: the eastern region

Junhua Liu 1/15/2017 2:52 PM
Deleted: 7

Junhua Liu 1/15/2017 2:52 PM
Deleted: 6

Junhua Liu 1/15/2017 2:52 PM
Deleted: 8

eastern equatorial Pacific; it extends southeastward to southern Africa and the south Indian Ocean. In this study, we use hindcast simulations from the GMI-CTM, driven by assimilated MERRA meteorological fields, to interpret and quantify the relative importance of the stratospheric input and surface emission to the interannual variations of tropospheric ozone over four sub-regions of the SHTOM from 1992 to 2011. Over the SHTOM region, IAV in the stratospheric contribution is found to be the most important factor driving the IAV of ozone, especially over the upper troposphere, where O_3 changes have strong radiative effects (Lacis et al., 1990). The IAV of the stratospheric contribution explains a large portion of variance in the tropospheric ozone especially during the austral winter season, even over two selected tropical regions. The strong influence of emission on ozone IAV is largely confined to the South Atlantic region in September.

Although the SHTOM looks like a continuous feature in the southern hemisphere, our study shows that the relative importance between stratospheric input and surface emissions changes over different subregions at different altitude. Over the two extra-tropics regions, the IAV of stratospheric contribution explains at least 50% of variance of the tropospheric ozone during its winter season. The IAV of ozone over the south Indian Ocean is dominantly driven by the IAV of stratospheric ozone contribution with little or no influence from surface emissions at 270 hPa and 430 hPa. Over the south Atlantic region, besides the stratospheric ozone input, the IAV of surface emissions from South America and southern Africa also play a big role on the IAV of ozone, especially in the lower levels. The influence from emission exceeds that from the stratospheric contribution on the ozone variability in September at 430 hPa. In December, the emission influence mainly from remote transport of pollutants from South and Southeast Asia is significant and stays high in the upper troposphere.

Compared to the extra-tropics regions, the influence from stratospheric input is smaller but still significant in two tropical regions at both 270 hPa and 430 hPa in August and September. Over tropical south Atlantic region, the IAV of stratospheric input plays a dominant role and explains 60% in August and 51% in September of the ozone IAV at 270 hPa. The stratospheric contribution is still significant at 430 hPa, but drops to less than half of that at 270 hPa. Emission contributions are not significant at these two levels,

Junhua Liu 12/31/2016 7:58 AM
Deleted: eastern region

Junhua Liu 1/15/2017 5:06 PM
Deleted: relatively

Junhua Liu 1/15/2017 5:07 PM
Deleted: and decreases with the decreasing altitude

Junhua Liu 1/15/2017 5:07 PM
Deleted: 64

Junhua Liu 1/15/2017 5:07 PM
Deleted: 52

Junhua Liu 2/2/2017 1:54 PM
Formatted: Font:Not Italic

Junhua Liu 12/31/2016 8:32 AM
Deleted: The stratospheric contribution drops to less than half of that at 270 hPa but is still significant at 430 hPa.

even during September. Our model shows that the IAV of ozone is partially driven by the IAV of lightning in September. In December, the changes in lightning NO_X have a significant impact on the ozone IAV, but show a negative correlation, which indicates that the transport and mixing of clean surface air exceeds ozone production from lightning NO_X emissions with a net negative impact of IAV in convection. Over the tropical southeastern Pacific, IAV in stratospheric input significantly affects the ozone IAV during these three months, explaining 28-40% of the variance of simulated ozone at 270 hPa. Emissions have little or no influence in August, September at 270 hPa and 430 hPa, but are significant in December at 270 hPa, explaining 17% of simulated ozone IAV. A further comparison of ozone and ENSO index shows that ENSO, which affects the tropical convection and large-scale upwelling, shows a strong negative correlation with the IAV of tropospheric ozone over this region. Therefore, the model simulations/predictions with different convective parameterizations exhibit large uncertainties over this region as observed in Stevenson et al. (2006) and Young et al. (2013).

In this study, our regional analysis based on the GMI-CTM model provides valuable conclusions on drivers of interannual variability over different subregions of the SHTOM and how they vary with the altitude. The quantification of their relative contributions on interannual time scales enhances our understanding of the IAV and, potentially, long-term trends in the tropospheric ozone and furthermore their effects on the radiative forcing of climate.

Junhua Liu 1/15/2017 5:08 PM
Deleted: 25-38

Junhua Liu 1/15/2017 5:08 PM
Deleted: 28

Junhua Liu 12/31/2016 8:34 AM
Deleted: to the

Junhua Liu 12/31/2016 8:34 AM
Deleted: radiative forcing change in climate

Acknowledgement

All model output used for this article can be obtained by contacting J. Liu (email: junhua.liu@nasa.gov). I gratefully acknowledge the financial support by NASA's Atmospheric Chemistry Modeling and Analysis Program (ACMAP) (grants NNH12ZDA001N). Work was performed under contract with NASA at Goddard. I would like to thank K. Pickering, L. Oman, A. Thompson, H. Liu for their helpful discussion.

References

Allen, D., Pickering, K., Duncan, B., and Damon, M.: Impact of lightning NO emissions on North American photochemistry as determined using the Global Modeling Initiative (GMI) model, Journal of Geophysical Research-Atmospheres, 115, 10.1029/2010jd014062, 2010.

Bals-Elsholz, T. M., Atallah, E. H., Bosart, L. F., Wasula, T. A., Cempa, M. J., and Lupo, A. R.: The wintertime Southern Hemisphere split jet: Structure, variability, and evolution, Journal of Climate, 14, 4191-4215, 10.1175/1520-0442(2001)014<4191:twshsj>2.0.co;2, 2001.

Bjerknes, J.: Atmospheric teleconnections from the equatorial Pacific, Mon. Weather Rev., 97(3), 163–172, 1969.

Chandra, S., Ziemke, J. R., Min, W., and Read, W. G.: Effects of 1997-1998 El Nino on tropospheric ozone and water vapor, Geophysical Research Letters, 25, 3867-3870, 10.1029/98gl02695, 1998.

Chandra, S., Ziemke, J. R., Bhartia, P. K., and Martin, R. V.: Tropical tropospheric ozone: Implications for dynamics and biomass burning, Journal of Geophysical Research-Atmospheres, 107, 10.1029/2001jd000447, 2002.

Chandra, S., Ziemke, J. R., Duncan, B. N., Diehl, T. L., Livesey, N. J., and Froidevaux, L.: Effects of the 2006 El Nino on tropospheric ozone and carbon monoxide: implications for dynamics and biomass burning, Atmospheric Chemistry and Physics, 9, 4239-4249, 2009.

Chen, Y., Randerson, J. T., Morton, D. C., DeFries, R. S., Collatz, G. J., Kasibhatla, P. S., Giglio, L., Jin, Y., and Marlier, M. E.: Forecasting Fire Season Severity in South America Using Sea Surface Temperature Anomalies, Science, 334, 787-791, 10.1126/science.1209472, 2011.

Chevan, A., and Sutherland, M.: HIERARCHICAL PARTITIONING, American Statistician, 45, 90-96, 10.2307/2684366, 1991.

Chin, M., Ginoux, P., Kinne, S., Torres, O., Holben, B. N., Duncan, B. N., Martin, R. V., Logan, J. A., Higurashi, A., and Nakajima, T.: Tropospheric aerosol optical thickness from the GOCART model and comparisons with satellite and Sun photometer measurements, J ATMOS SCI, 59, 461-483, 2002.

Danielsen, E. F.: Stratospheric-Tropospheric Exchange Based on Radioactivity, Ozone and Potential VorticityStratospheric-Tropospheric Exchange Based on Radioactivity, Ozone and Potential Vorticity, Journal of the Atmospheric Sciences, 25, 502-518, 10.1175/1520-0469(1968).

Doherty, R. M., Stevenson, D. S., Johnson, C. E., Collins, W. J., and Sanderson, M. G.: Tropospheric ozone and El Nino-Southern Oscillation: Influence of atmospheric dynamics, biomass burning emissions, and future climate change, Journal of Geophysical Research-Atmospheres, 111, 10.1029/2005jd006849, 2006.

Duncan, B. N., Martin, R. V., Staudt, A. C., Yevich, R., and Logan, J. A.: Interannual and seasonal variability of biomass burning emissions constrained by satellite observations, Journal of Geophysical Research-Atmospheres, 108, 10.1029/2002jd002378, 2003.

Duncan, B. N., Strahan, S. E., Yoshida, Y., Steenrod, S. D., and Livesey, N.: Model study of the cross-tropopause transport of biomass burning pollution, ATMOS CHEM PHYS, 7, 3713-3736, 2007.
Eyring, V., Lamarque, J.-F., Hess, P., Arfeuille, F., Bowman, K., Chipperfield, M. P., Duncan, B., Fiore, A., Gettelman, A., Giorgetta, M. A., Granier, C., Kinnison, M. H. D., Kunze, M., Langematz, U., Luo, B., Martin, R., Matthes, K., Newman, P. A., Peter, T., Robock, A., Ryerson, T., Saiz-Lopez, A., Salawitch, R., Schultz, M., Shepherd, T. G., Shindell, D., Staehelin, J., Tegtmeier, S., Thomason, L., Tilmes, S., Vernier, J.-P., Waugh, D. W., and Young, P. J.: Overview of IGAC/SPARC Chemistry-Climate Model Initiative (CCMI) Community Simulations in Support of Upcoming Ozone and Climate Assessments. In: SPARC Newsletter 40, 48, WMO/SPARC, Zürich, 2013.
Fishman, J., Watson, C. E., Larsen, J. C., and Logan, J. A.: DISTRIBUTION OF TROPOSPHERIC OZONE DETERMINED FROM SATELLITE DATA, Journal of Geophysical Research-Atmospheres, 95, 3599-3617, 10.1029/JD095iD04p03599, 1990.
Folkins, I., Braun, C., Thompson, A. M., and Witte, J.: Tropical ozone as an indicator of deep convection, Journal of Geophysical Research-Atmospheres, 107, 10.1029/2001jd001178, 2002.
Groemping, U.: Two simple estimators of relative importance in linear regression based on variance decomposition - Response, American Statistician, 61, 282-283, 2007.
Guenther, A., Karl, T., Harley, P., Wiedinmyer, C., Palmer, P. I., and Geron, C.: Estimates of global terrestrial isoprene emissions using MEGAN (Model of Emissions of Gases and Aerosols from Nature), ATMOS CHEM PHYS, 6, 3181-3210, 2006.
Hess, P., and Mahowald, N.: Interannual variability in hindcasts of atmospheric chemistry: the role of meteorology, ATMOS CHEM PHYS, 9, 5261-5280, 10.5194/acp-9-5261-2009, 2009.
Hoskins, B. J., and Rodwell, M. J.: A MODEL OF THE ASIAN SUMMER MONSOON .1. THE GLOBAL-SCALE, Journal of the Atmospheric Sciences, 52, 1329-1340, 10.1175/1520-0469(1995)052<1329:amotas>2.0.co;2, 1995.
Jacob, D. J., Heikes, B. G., Fan, S. M., Logan, J. A., Mauzerall, D. L., Bradshaw, J. D., Singh, H. B., Gregory, G. L., Talbot, R. W., Blake, D. R., and Sachse, G. W.: Origin of ozone and NOx in the tropical troposphere: A photochemical analysis of aircraft observations over the South Atlantic basin, Journal of Geophysical Research-Atmospheres, 101, 24235-24250, 10.1029/96jd00336, 1996.
Jenkins, G. S., and Ryu, J. H.: Space-borne observations link the tropical atlantic ozone maximum and paradox to lightning, Atmospheric Chemistry and Physics, 4, 361-375, 2004a.
Jenkins, G. S., and Ryu, J. H.: Linking horizontal and vertical transports of biomass fire emissions to the tropical Atlantic ozone paradox during the Northern Hemisphere winter season: climatology, Atmospheric Chemistry and Physics, 4, 449-469, 2004b.
Jourdain, L., Worden, H. M., Worden, J. R., Bowman, K., Li, Q., Eldering, A., Kulawik, S. S., Osterman, G., Boersma, K. F., Fisher, B., Rinsland, C. P., Beer, R., and Gunson, M.: Tropospheric vertical distribution of tropical Atlantic ozone

observed by TES during the northern African biomass burning season, Geophysical Research Letters, 34, 10.1029/2006gl028284, 2007.

Julian, P. R., and Chervin, R. M.: A study of the Southern Oscillation and Walker Circulation phenomenon, Mon. Weather Rev., 106(10), 1433–1451, 1978.

Karoly, D. J., Vincent, D. G., and Schrage, J. M.: Meteorology of the Southern Hemisphere, General circulation, American Meteorological Society, 45 Beacon St., Boston, MA, 02108, 1998.

Kim, P. S., Jacob, D. J., Liu, X., Warner, J. X., Yang, K., Chance, K., Thouret, V., and Nedelec, P.: Global ozone-CO correlations from OMI and AIRS: constraints on tropospheric ozone sources, Atmospheric Chemistry and Physics, 13, 9321-9335, 10.5194/acp-13-9321-2013, 2013.

Kruskal, W.: RELATIVE IMPORTANCE BY AVERAGING OVER ORDERINGS, American Statistician, 41, 6-10, 10.2307/2684310, 1987.

Lacis, A. A., Wuebbles, D. J., and Logan, J. A.: RADIATIVE FORCING OF CLIMATE BY CHANGES IN THE VERTICAL-DISTRIBUTION OF OZONE, Journal of Geophysical Research-Atmospheres, 95, 9971-9981, 10.1029/JD095iD07p09971, 1990.

Lawrence, M. G., von Kuhlmann, R., Salzmann, M., and Rasch, P. J.: The balance of effects of deep convective mixing on tropospheric ozone, Geophysical Research Letters, 30, 10.1029/2003gl017644, 2003.

Lewis, S. L., Brando, P. M., Phillips, O. L., van der Heijden, G. M. F., and Nepstad, D.: The 2010 Amazon Drought, Science, 331, 554-554, 10.1126/science.1200807, 2011.

Lin, M., Fiore, A. M., Cooper, O. R., Horowitz, L. W., Langford, A. O., Levy II, H., Johnson, B. J., Vaishali Naik, V., Oltmans, S. J., and Senff, C. J.: Springtime high surface ozone events over the western United States: Quantifying the role of stratospheric intrusions, Submitted to JGR-Atmosphere, CalNex Special Section, 2012.

Liu, J., Logan, J. A., Jones, D. B. A., Livesey, N. J., Megretskaia, I., Carouge, C., and Nedelec, P.: Analysis of CO in the tropical troposphere using Aura satellite data and the GEOS-Chem model: insights into transport characteristics of the GEOS meteorological products, Atmospheric Chemistry and Physics, 10, 12207-12232, 10.5194/acp-10-12207-2010, 2010.

Liu, J., Logan, J. A., Murray, L. T., Pumphrey, H. C., Schwartz, M. J., and Megretskaia, I. A.: Transport analysis and source attribution of seasonal and interannual variability of CO in the tropical upper troposphere and lower stratosphere, Atmospheric Chemistry and Physics, 13, 129-146, 10.5194/acp-13-129-2013, 2013.

Liu, J., Rodriguez, J. M., Thompson, A. M., Logan, J. A., Douglass, A. R., Olsen, M. A., Steenrod, S. D., and Posny, F.: Origins of tropospheric ozone interannual variation over Reunion: A model investigation, Journal of Geophysical Research-Atmospheres, 121, 521-537, 10.1002/2015jd023981, 2016.

Logan, J. A., Prather, M. J., Wofsy, S. C., and McElroy, M. B.: TROPOSPHERIC CHEMISTRY - A GLOBAL PERSPECTIVE, Journal of Geophysical Research-Oceans and Atmospheres, 86, 7210-7254, 10.1029/JC086iC08p07210, 1981.

Logan, J. A., Megretskaia, I., Nassar, R., Murray, L. T., Zhang, L., Bowman, K. W., Worden, H. M., and Luo, M.: Effects of the 2006 El Nino on tropospheric composition as revealed by data from the Tropospheric Emission Spectrometer (TES), Geophysical Research Letters, 35, 10.1029/2007gl031698, 2008.

Martin, R. V., Jacob, D. J., Logan, J. A., Bey, I., Yantosca, R. M., Staudt, A. C., Li, Q. B., Fiore, A. M., Duncan, B. N., Liu, H. Y., Ginoux, P., and Thouret, V.: Interpretation of TOMS observations of tropical tropospheric ozone with a global model and in situ observations, Journal of Geophysical Research-Atmospheres, 107, 10.1029/2001jd001480, 2002.

Murray, L. T., Logan, J. A., and Jacob, D. J.: Interannual variability in tropical tropospheric ozone and OH: The role of lightning, Journal of Geophysical Research-Atmospheres, 118, 11468-11480, 10.1002/jgrd.50857, 2013.

Nakamura, H., and Shimpo, A.: Seasonal Variations in the Southern Hemisphere Storm Tracks and Jet Streams as Revealed in a Reanalysis Dataset., *J. Climate*, **17**, 1828–1844., 2004.

Neu, J. L., Flury, T., Manney, G. L., Santee, M. L., Livesey, N. J., and Worden, J.: Tropospheric ozone variations governed by changes in stratospheric circulation, Nature Geoscience, 7, 340-344, 10.1038/ngeo2138, 2014.

Olivier, J. G. J., Van Aardenne, J. A., Dentener, F. J., Pagliari, V., Ganzeveld, L. N., and Peters, J. A. H. W.: Recent trends in global greenhouse gas emissions: regional trends and spatial distribution of key sources, in: Non-CO2 Greenhouse Gases (NCGG-4), coordinator: van Amstel, A., Millpress, Rotterdam, ISBN 905966 043 9, 325–330,, 2005.

Olsen, M. A., Wargan, K., and Pawson, S.: Tropospheric column ozone response to ENSO in GEOS-5 assimilation of OMI and MLS ozone data, Atmospheric Chemistry and Physics, 16, 7091-7103, 10.5194/acp-16-7091-2016, 2016.

Oman, L. D., Ziemke, J. R., Douglass, A. R., Waugh, D. W., Lang, C., Rodriguez, J. M., and Nielsen, J. E.: The response of tropical tropospheric ozone to ENSO, Geophysical Research Letters, 38, 10.1029/2011gl047865, 2011.

Oman, L. D., Douglass, A. R., Ziemke, J. R., Rodriguez, J. M., Waugh, D. W., and Nielsen, J. E.: The ozone response to ENSO in Aura satellite measurements and a chemistry-climate simulation, Journal of Geophysical Research-Atmospheres, 118, 965-976, 10.1029/2012jd018546, 2013.

Pickering, K. E., Thompson, A. M., Tao, W. K., and Kucsera, T. L.: UPPER TROPOSPHERIC OZONE PRODUCTION FOLLOWING MESOSCALE CONVECTION DURING STEP EMEX, Journal of Geophysical Research-Atmospheres, 98, 8737-8749, 10.1029/93jd00875, 1993.

Pickering, K. E., Thompson, A. M., Wang, Y. S., Tao, W. K., McNamara, D. P., Kirchhoff, V., Heikes, B. G., Sachse, G. W., Bradshaw, J. D., Gregory, G. L., and Blake, D. R.: Convective transport of biomass burning emissions over Brazil during TRACE A, Journal of Geophysical Research-Atmospheres, 101, 23993-24012, 10.1029/96jd00346, 1996.

Prather, M. J., Zhu, X., Tang, Q., Hsu, J. N., and Neu, J. L.: An atmospheric chemist in search of the tropopause, J GEOPHYS RES-ATMOS, 116, D04306, 10.1029/2010jd014939, 2011.

Rienecker, M. M., Suarez, M. J., Gelaro, R., Todling, R., Bacmeister, J., Liu, E., Bosilovich, M. G., Schubert, S. D., Takacs, L., Kim, G.-K., Bloom, S., Chen, J., Collins, D., Conaty, A., Da Silva, A., Gu, W., Joiner, J., Koster, R. D., Lucchesi, R., Molod, A., Owens, T., Pawson, S., Pegion, P., Redder, C. R., Reichle, R., Robertson, F. R., Ruddick, A. G., Sienkiewicz, M., and Woollen, J.: MERRA: NASA's Modern-Era Retrospective Analysis for Research and Applications, Journal of Climate, 24, 3624-3648, 10.1175/jcli-d-11-00015.1, 2011.

Rodwell, M. J., and Hoskins, B. J.: Subtropical anticyclones and summer monsoons, Journal of Climate, 14, 3192-3211, 10.1175/1520-0442(2001)014<3192:saasm>2.0.co;2, 2001.

Sauvage, B., Thouret, V., Thompson, A. M., Witte, J. C., Cammas, J. P., Nedelec, P., and Athier, G.: Enhanced view of the "tropical Atlantic ozone paradox" and "zonal wave one" from the in situ MOZAIC and SHADOZ data, Journal of Geophysical Research-Atmospheres, 111, 10.1029/2005jd006241, 2006.

Sauvage, B., Martin, R. V., van Donkelaar, A., and Ziemke, J. R.: Quantification of the factors controlling tropical tropospheric ozone and the South Atlantic maximum, Journal of Geophysical Research-Atmospheres, 112, 10.1029/2006jd008008, 2007.

Solomon, S., Thompson, D. W. J., Portmann, R. W., Oltmans, S. J., and Thompson, A. M.: On the distribution and variability of ozone in the tropical upper troposphere: Implications for tropical deep convection and chemical-dynamical coupling, Geophysical Research Letters, 32, 10.1029/2005gl024323, 2005.

Stevenson, D. S., Dentener, F. J., Schultz, M. G., Ellingsen, K., van Noije, T. P. C., Wild, O., Zeng, G., Amann, M., Atherton, C. S., Bell, N., Bergmann, D. J., Bey, I., Butler, T., Cofala, J., Collins, W. J., Derwent, R. G., Doherty, R. M., Drevet, J., Eskes, H. J., Fiore, A. M., Gauss, M., Hauglustaine, D. A., Horowitz, L. W., Isaksen, I. S. A., Krol, M. C., Lamarque, J. F., Lawrence, M. G., Montanaro, V., Muller, J. F., Pitari, G., Prather, M. J., Pyle, J. A., Rast, S., Rodriguez, J. M., Sanderson, M. G., Savage, N. H., Shindell, D. T., Strahan, S. E., Sudo, K., and Szopa, S.: Multimodel ensemble simulations of present-day and near-future tropospheric ozone, Journal of Geophysical Research-Atmospheres, 111, 10.1029/2005jd006338, 2006.

Stohl, A., Bonasoni, P., Cristofanelli, P., Collins, W., Feichter, J., Frank, A., Forster, C., Gerasopoulos, E., Gaggeler, H., James, P., Kentarchos, T., Kromp-Kolb, H., Kruger, B., Land, C., Meloen, J., Papayannis, A., Priller, A., Seibert, P., Sprenger, M., Roelofs, G. J., Scheel, H. E., Schnabel, C., Siegmund, P., Tobler, L., Trickl, T., Wernli, H., Wirth, V., Zanis, P., and Zerefos, C.: Stratosphere-troposphere exchange: A review, and what we have learned from STACCATO, Journal of Geophysical Research-Atmospheres, 108, 10.1029/2002jd002490, 2003.

Strahan, S. E., Duncan, B. N., and Hoor, P.: Observationally derived transport diagnostics for the lowermost stratosphere and their application to the GMI chemistry and transport model, ATMOS CHEM PHYS, 7, 2435-2445, 2007.

Strahan, S. E., Douglass, A. R., and Newman, P. A.: The contributions of chemistry and transport to low arctic ozone in March 2011 derived from Aura MLS observations, Journal of Geophysical Research-Atmospheres, 118, 1563-1576, 10.1002/jgrd.50181, 2013.

Strode, S. A., Rodriguez, J. M., Logan, J. A., Cooper, O. R., Witte, J. C., Lamsal, L. N., Damon, M., Van Aartsen, B., Steenrod, S. D., and Strahan, S. E.: Trends and variability in surface ozone over the United States, Journal of Geophysical Research-Atmospheres, 120, 9020-9042, 10.1002/2014jd022784, 2015.
Sudo, K., and Takahashi, M.: Simulation of tropospheric ozone changes during 1997-1998 El Nino: Meteorological impact on tropospheric photochemistry, Geophysical Research Letters, 28, 4091-4094, 10.1029/2001gl013335, 2001.
Thompson, A. M., Pickering, K. E., McNamara, D. P., Schoeberl, M. R., Hudson, R. D., Kim, J. H., Browell, E. V., Kirchhoff, V., and Nganga, D.: Where did tropospheric ozone over southern Africa and the tropical Atlantic come from in October 1992? Insights from TOMS, GTE TRACE A, and SAFARI 1992, Journal of Geophysical Research-Atmospheres, 101, 24251-24278, 10.1029/96jd01463, 1996.
Thompson, A. M., Witte, J. C., McPeters, R. D., Oltmans, S. J., Schmidlin, F. J., Logan, J. A., Fujiwara, M., Kirchhoff, V., Posny, F., Coetzee, G. J. R., Hoegger, B., Kawakami, S., Ogawa, T., Johnson, B. J., Vomel, H., and Labow, G.: Southern Hemisphere Additional Ozonesondes (SHADOZ) 1998-2000 tropical ozone climatology - 1. Comparison with Total Ozone Mapping Spectrometer (TOMS) and ground-based measurements, Journal of Geophysical Research-Atmospheres, 108, 10.1029/2001jd000967, 2003.
Thouret, V., Saunois, M., Minga, A., Mariscal, A., Sauvage, B., Solete, A., Agbangla, D., Nedelec, P., Mari, C., Reeves, C. E., and Schlager, H.: An overview of two years of ozone radio soundings over Cotonou as part of AMMA, Atmospheric Chemistry and Physics, 9, 6157-6174, 2009.
Tocquer, F., Barret, B., Mari, C., Le Flochmoen, E., Cammas, J. P., and Sauvage, B.: An upper tropospheric 'ozone river' from Africa to India during the 2008 Asian post-monsoon season, Tellus Series B-Chemical and Physical Meteorology, 67, 10.3402/tellusb.v67.25350, 2015.
van der Werf, G. R., Randerson, J. T., Giglio, L., Collatz, G. L., Mu, M., Kasibhatla, P. S., Morton, D. C., DeFries, R. S., Jin, Y., and T.T., v. L.: Global fire emissions and the contribution of deforestation, savanna, forest, agricultural, and peat fires (1997–2009), ATMOS CHEM PHYS, 10, 16153-16230, 2010.
Voulgarakis, A., Savage, N. H., Wild, O., Braesicke, P., Young, P. J., Carver, G. D., and Pyle, J. A.: Interannual variability of tropospheric composition: the influence of changes in emissions, meteorology and clouds, Atmospheric Chemistry and Physics, 10, 2491-2506, 10.5194/acp-10-2491-2010, 2010.
Voulgarakis, A., Hadjinicolaou, P., and Pyle, J. A.: Increases in global tropospheric ozone following an El Nino event: examining stratospheric ozone variability as a potential driver, Atmospheric Science Letters, 12, 228-232, 10.1002/asl.318, 2011.
Voulgarakis, A., Marlier, M. E., Faluvegi, G., Shindell, D. T., Tsigaridis, K., and Mangeon, S.: Interannual variability of tropospheric trace gases and aerosols: The role of biomass burning emissions, Journal of Geophysical Research-Atmospheres, 120, 7157-7173, 10.1002/2014jd022926, 2015.
Wargan, K., Pawson, S., Olsen, M. A., Witte, J. C., Douglass, A. R., Ziemke, J. R., Strahan, S. E., and Nielsen, J. E.: The global structure of upper troposphere-lower

stratosphere ozone in GEOS-5: A multiyear assimilation of EOS Aura data, Journal of Geophysical Research-Atmospheres, 120, 2013-2036, 10.1002/2014jd022493, 2015.

Weller, R., Lilischkis, R., Schrems, O., Neuber, R., and Wessel, S.: Vertical ozone distribution in the marine atmosphere over the central Atlantic Ocean (56 degrees S 50 degrees N), Journal of Geophysical Research-Atmospheres, 101, 1387-1399, 10.1029/95jd02838, 1996.

WMO: Scientific Assessment of Ozone Depletion: 2014, Global Ozone Research and Monitoring Project, World Meteorological Organization, Geneva, Switzerland, 2014.

Zeng, G., and Pyle, J. A.: Influence of El Nino Southern Oscillation on stratosphere/troposphere exchange and the global tropospheric ozone budget, Geophysical Research Letters, 32, 10.1029/2004gl021353, 2005.

Ziemke, J. R., Chandra, S., Thompson, A. M., and McNamara, D. P.: Zonal asymmetries in southern hemisphere column ozone: Implications of biomass burning, Journal of Geophysical Research-Atmospheres, 101, 14421-14427, 10.1029/96jd01057, 1996.

Ziemke, J. R., and Chandra, S.: La Nina and El Nino-induced variabilities of ozone in the tropical lower atmosphere during 1970-2001, Geophysical Research Letters, 30, 10.1029/2002gl016387, 2003.

Ziemke, J. R., Chandra, S., Oman, L. D., and Bhartia, P. K.: A new ENSO index derived from satellite measurements of column ozone, Atmospheric Chemistry and Physics, 10, 3711-3721, 2010.

Ziemke, J. R., Olsen, M. A., Witte, J. C., Douglass, A. R., Strahan, S. E., Wargan, K., Liu, X., Schoeberl, M. R., Yang, K., Kaplan, T. B., Pawson, S., Duncan, B. N., Newman, P. A., Bhartia, P. K., and Heney, M. K.: Assessment and applications of NASA ozone data products derived from Aura OMI/MLS satellite measurements in context of the GMI chemical transport model, Journal of Geophysical Research-Atmospheres, 119, 5671-5699, 10.1002/2013jd020914, 2014.

Ziemke, J.R., A.R. Douglass, L.D. Oman, S.E. Strahan, and B.N. Duncan, "Tropospheric ozone variability in the tropics from ENSO to MJO and shorter timescales", Atmos. Chem. Phys. Discuss., 15, 6373-6401, doi:10.5194/acpd-15-6373-2015, 2015.

Figures:

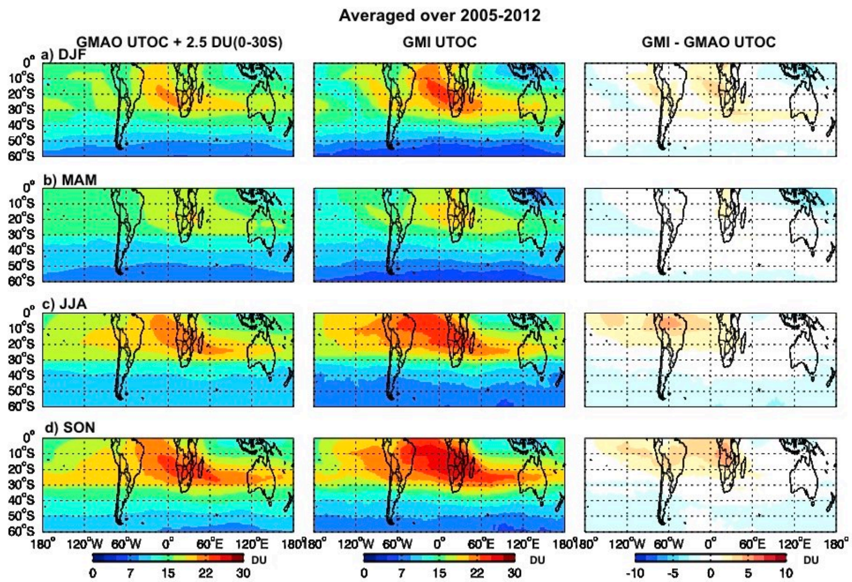

Figure 1: Seasonal climatology of upper tropospheric column ozone (UTOC, integrated from 500 hPa to the tropopause) (in Dobson Units) for (a) December-January-February (DJF), (b) March-April-May (MAM), (c) June-July-August (JJA), and (d) September-October-November (SON) averaged from 2005 to 2012 for GMAO assimilated ozone (left) and GMI-CTM Hindcast-VE ozone (middle) and their absolute difference (right). The GMAO assimilated ozone has been adjusted by adding 2.5 DU in 0-30° S based on Wargan et al. (2015).

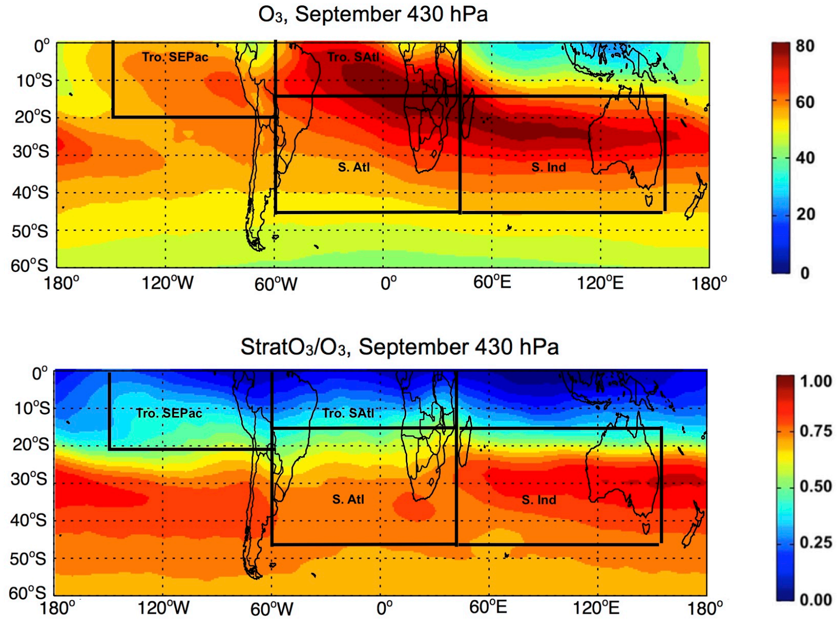

Figure 2: The simulated ozone (top) and the $StratO_3/O_3$ (bottom) at 430 hPa averaged over 1992-2011 in September. Stronger stratospheric influence happens over southern hemisphere centered on 30° S, co-locating with subtropical jet stream regions with descending stratospheric air. The black boxes show four regions discussed in this study. From left to right: (1) Tropical southeastern Pacific (0-20° S, 150° W-60° W); (2) Tropical South Atlantic region (0-15° S, 60° W-40° E); (3) Subtropical South Atlantic region (15° S-45° S, 60° W-40° E); (4) Subtropical South Indian Ocean (15° S-45° S, 40° E-150° E).

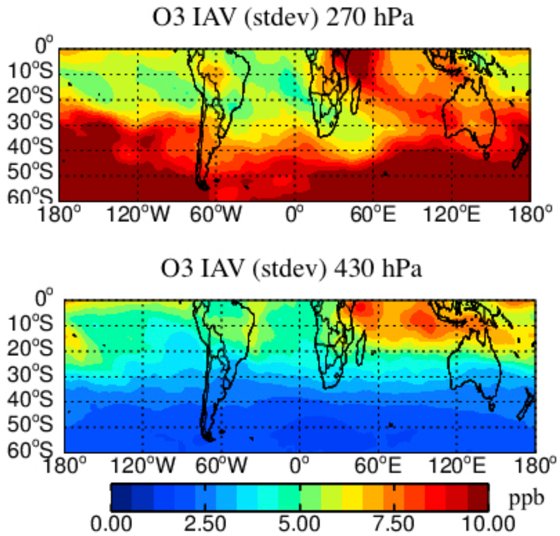

Figure 3: The interannual variations (IAV, unit of ppb) of simulated ozone at 270 hPa (top) and 430 hPa (bottom). The standard deviation of ozone anomalies (removing the monthly mean) over 1991-2011 represents the IAV.

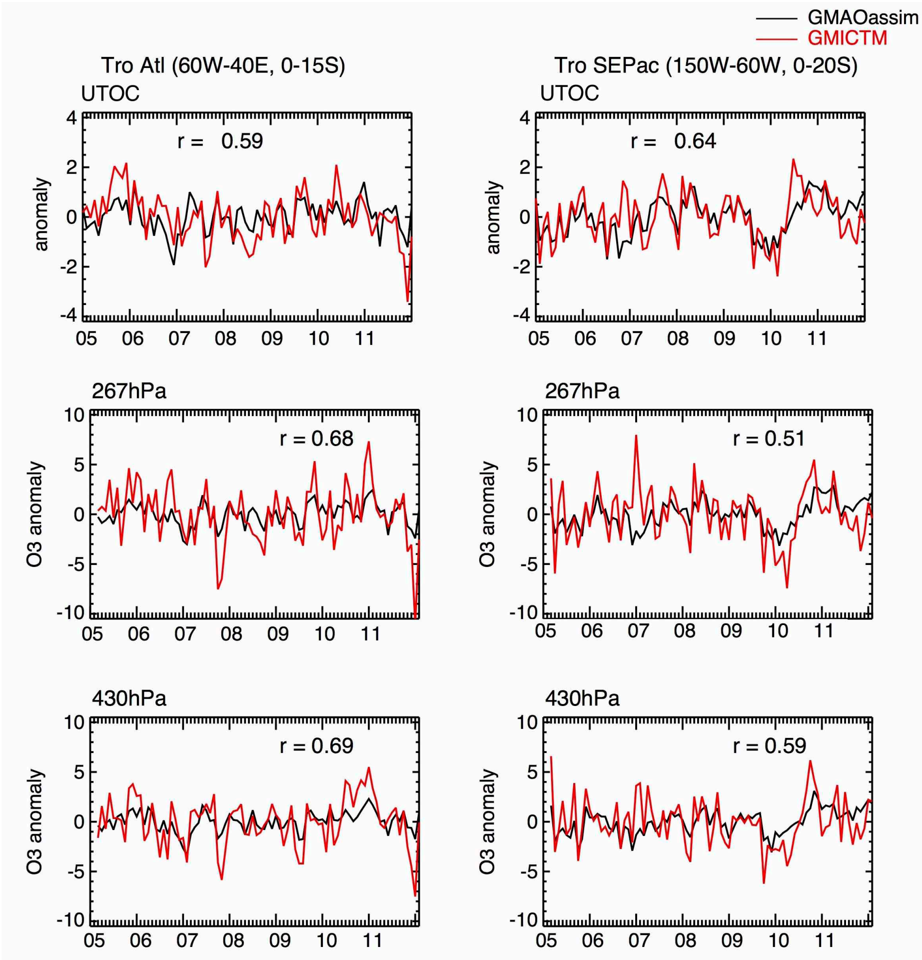

Figure 4: Time series plots of upper tropospheric ozone column (UTOC, integrated from 500 hPa to the tropopause; unit: DU) anomalies and tropospheric ozone anomalies (unit: ppb) at 270 hPa and 430 hPa from GMAO assimilated data (black) and GMI-CTM (red) over (left) Tropical South Atlantic region (0-15° S, 60° W-40° E); (right) Tropical southeastern Pacific (0-20° S, 150° W-60° W) from 2005 to 2011. The anomalies are calculated by removing the monthly mean averaged from 2005 to 2011.

Junhua Liu 1/15/2017 2:57 PM
Deleted: 3

Junhua Liu 1/10/2017 3:03 PM
Deleted: at 270 hPa and 430 hPa

Junhua Liu 1/10/2017 3:03 PM
Deleted: and upper tropospheric ozone column (UTOC, integrated from 500 hPa to the tropopause) anomalies o

Junhua Liu 2/2/2017 1:54 PM
Formatted: Font:9 pt, Bold

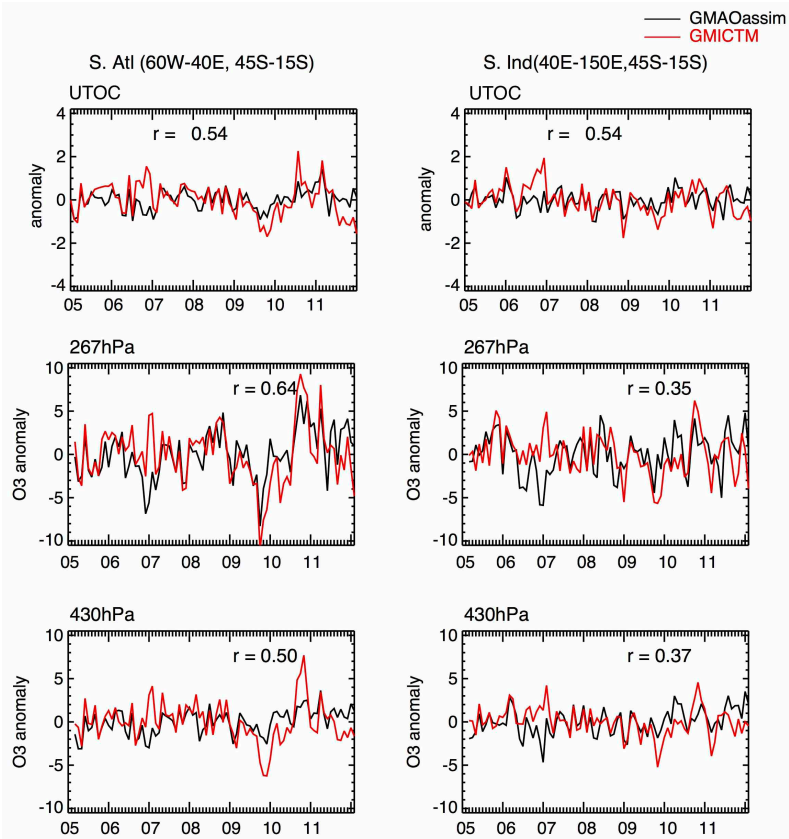

Figure 5: Time series plots of upper tropospheric ozone column (UTOC, integrated from 500 hPa to the tropopause; unit: DU) anomalies and tropospheric ozone anomalies (unit: ppb) at 270 hPa and 430 hPa from GMAO assimilated data (black) and GMI-CTM (red) over (left) South Atlantic (15° S-45° S, 60° W-40° E); (right) South Indian Ocean (15° S-45° S, 40° E-150° E) from 2005 to 2011. The anomalies are calculated by removing the monthly mean averaged from 2005 to 2011.

Junhua Liu 1/15/2017 2:57 PM
Deleted: 4

Junhua Liu 1/10/2017 3:04 PM
Deleted: at 270 hPa and 430 hPa and upper tropospheric ozone column (UTOC, integrated from 500 hPa to the tropopause) anomalies

Junhua Liu 2/2/2017 1:54 PM
Formatted: Font:9 pt, Bold

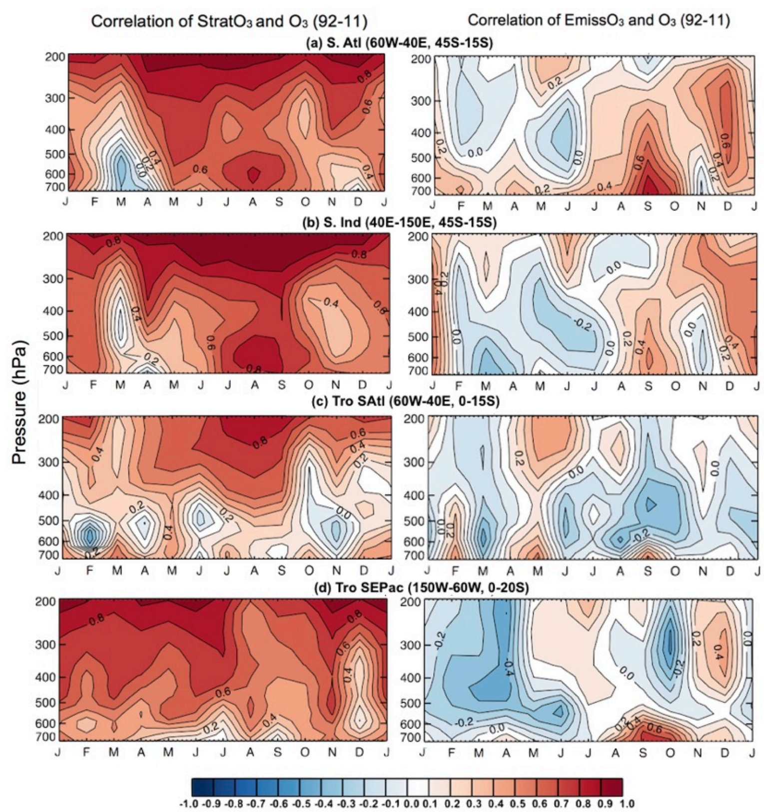

Figure 6: Monthly profile maps of correlations coefficients between ozone and left) $StratO_3$, right) $EmissO_3$ from 1992 to 2011 over (a) South Atlantic (15° S-45° S, 60° W-40° E); (b) South Indian Ocean (15° S-45° S, 40° E-150° E); c) Tropical South Atlantic region (0-15° S, 60° W-40° E); d) Tropical southeastern Pacific (0-20° S, 150° W-60° W). Y-axis is pressure in unit hPa.

Junhua Liu 1/15/2017 2:57 PM
Deleted: 5

Junhua Liu 2/2/2017 1:54 PM
Formatted: Font:9 pt, Bold

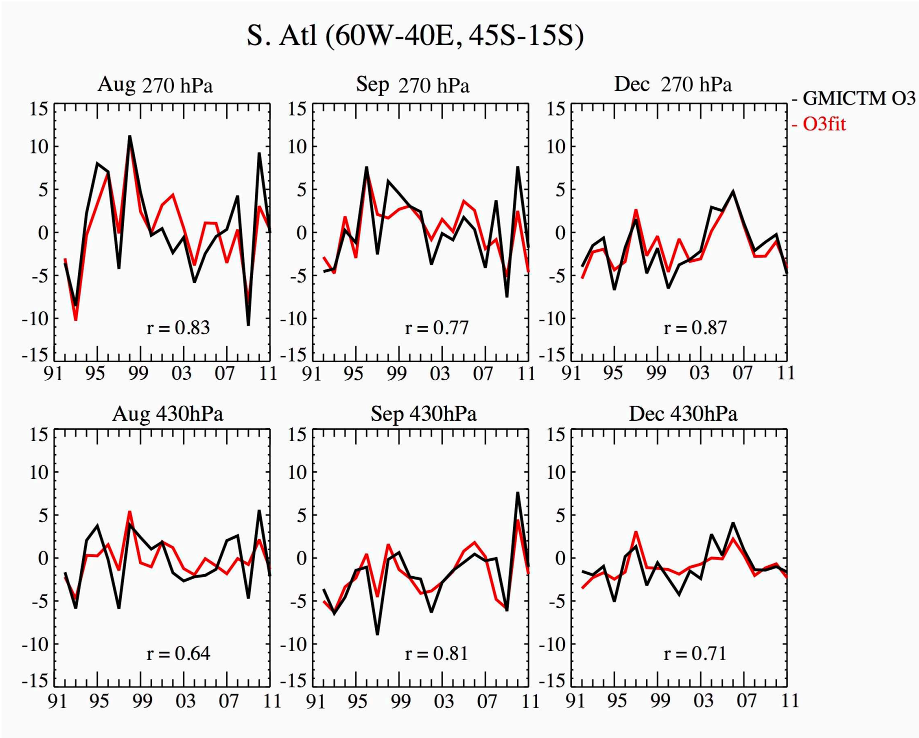

Figure 7: Comparison of the simulated ozone anomalies and the calculated ozone anomalies relying on two predictor variables: $StratO_3$, $EmissO_3$ at 270 hPa and 430 hPa over South Atlantic region. Three panels show results from August (left), September (middle) and December (right) from 1992 to 2011. Unit for y-axis is ppb.

Junhua Liu 1/15/2017 2:57 PM
Deleted: 6

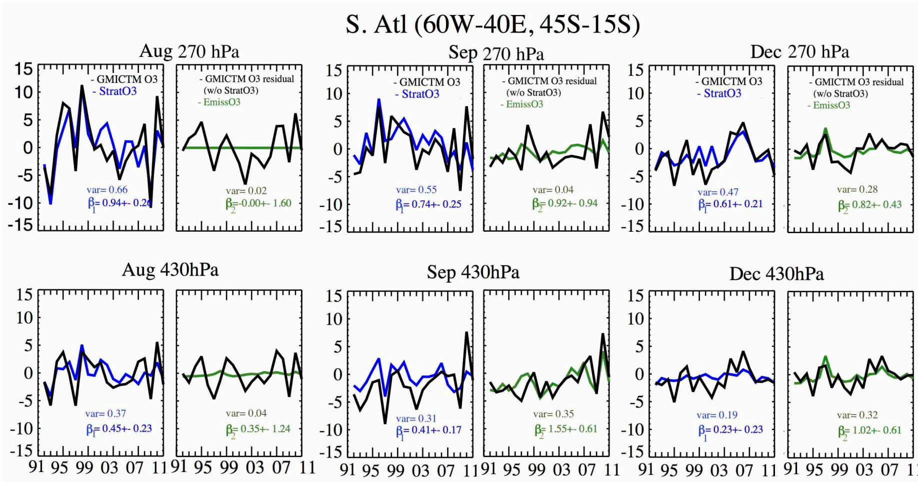

Figure 8: The multi-regression results of simulated ozone anomalies over South Atlantic region relying on two predictor variables: StratO$_3$ (blue), EmissO$_3$ (green) at 270 hPa and 430 hPa. Three panels show results from August (left), September (middle) and December (right) from 1992 to 2011. Each panel contains two columns. The left column of each panel compares the anomalies of StratO$_3$ (blue) and simulated ozone mixing ratio (black) from the GMI-CTM model at 270 and 430 hPa. The right column compares the simulated O$_3$ residual after removing the regression from StratO$_3$ (black line) and EmissO$_3$ (green line) at these two levels. EmissO$_3$ is calculated from the difference of simulated ozone between the run with yearly-varied emission and the run with constant emission. Unit for y-axis is ppb. The variance explained by each predictor (var), regression coefficient (β) and its 95% confidence level are labeled in each panel.

Junhua Liu 1/15/2017 2:57 PM
Deleted: 7

Junhua Liu 1/15/2017 12:38 PM
Deleted: correlation (r)

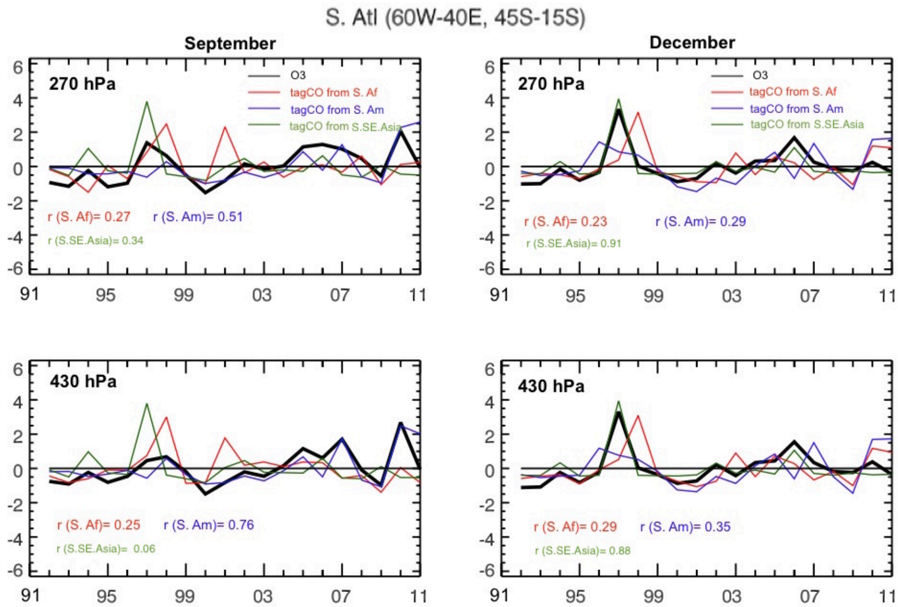

Figure 9: The standardized anomalies of the tagged CO tracers over South Atlantic from three burning source regions, including southern Africa (red), South America (blue) and South and Southeast Asia (green) and their comparison with the EmissO$_3$ (black) at 270 and 430 hPa in September and December from 1992 to 2011.

Junhua Liu 1/15/2017 2:57 PM
Deleted: 8

Junhua Liu 12/31/2016 7:59 AM
Deleted: eastern region

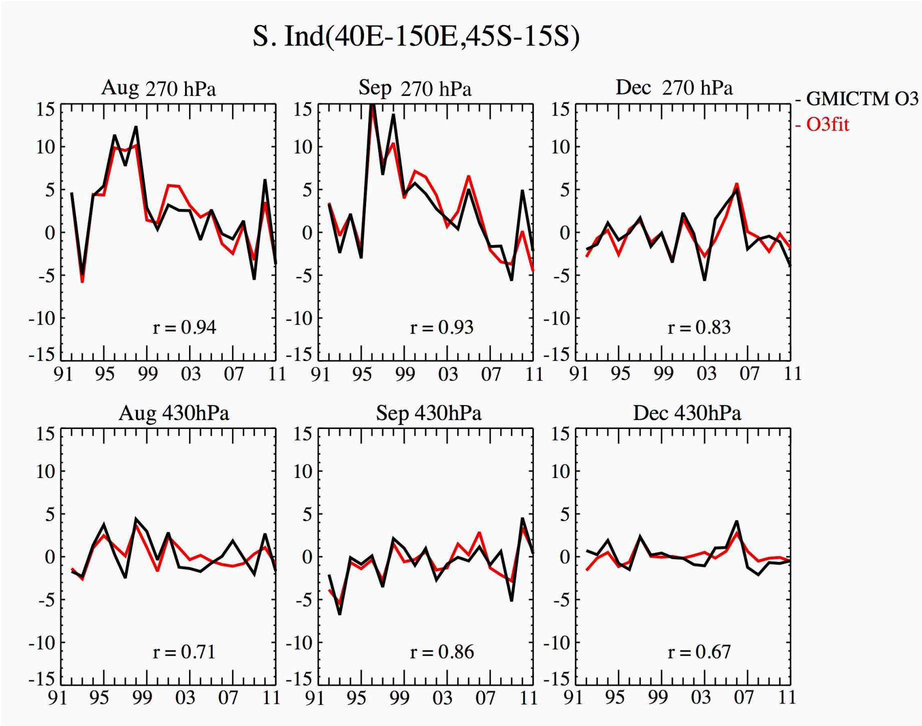

Figure 10: Comparison of the simulated ozone anomalies and the reconstructed ozone anomalies relying on two predictor variables: $StratO_3$, $EmissO_3$ at 270 hPa and 430 hPa over South Indian Ocean region. Three panels show results from August (left), September (middle) and December (right) from 1992 to 2011. Unit for y-axis is ppb.

Junhua Liu 1/15/2017 2:57 PM
Deleted: 9

Junhua Liu 2/2/2017 1:54 PM
Formatted: Font:Underline color: Auto, Font color: Auto

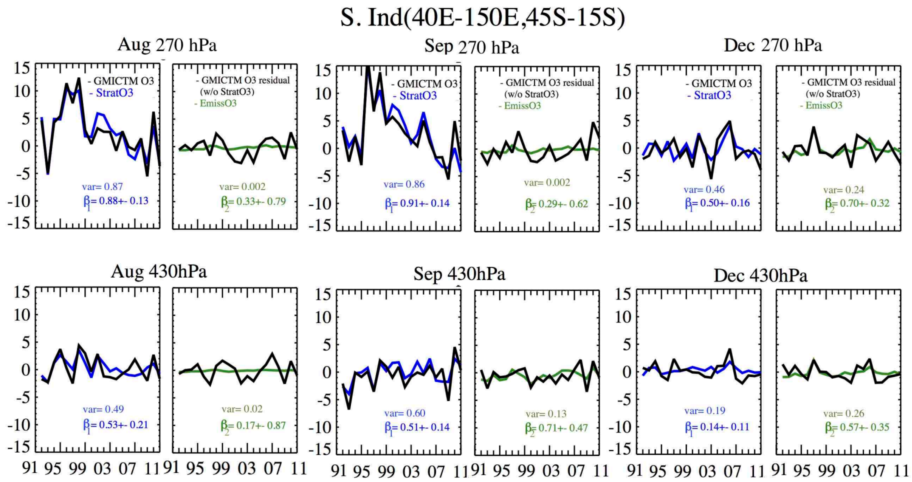

Figure 11: The multi-regression results of simulated ozone anomalies over South Indian Ocean region relying on two predictor variables: $StratO_3$ (blue), $EmissO_3$ (green) at 270 hPa and 430 hPa. Three panels show results from August (left), September (middle) and December (right) from 1992 to 2011. Each panel contains two columns. The left column of each panel compares the anomalies of $StratO_3$ (blue) and simulated ozone mixing ratio (black) from the GMI-CTM model at 270 and 430 hPa. The right column compares the simulated O_3 residual after removing the regression from $StratO_3$ (black line) and $EmissO_3$ (green line) at these two levels. $EmissO_3$ is calculated from the difference of simulated ozone between the run with yearly-varied emission and the run with constant emission. Unit for y-axis is ppb. The variance explained by each predictor (var), regression coefficient (β) and its 95% confidence level are labeled in each panel.

Junhua Liu 1/15/2017 2:57 PM
Deleted: 0

Junhua Liu 1/15/2017 12:40 PM
Deleted: correlation (r),

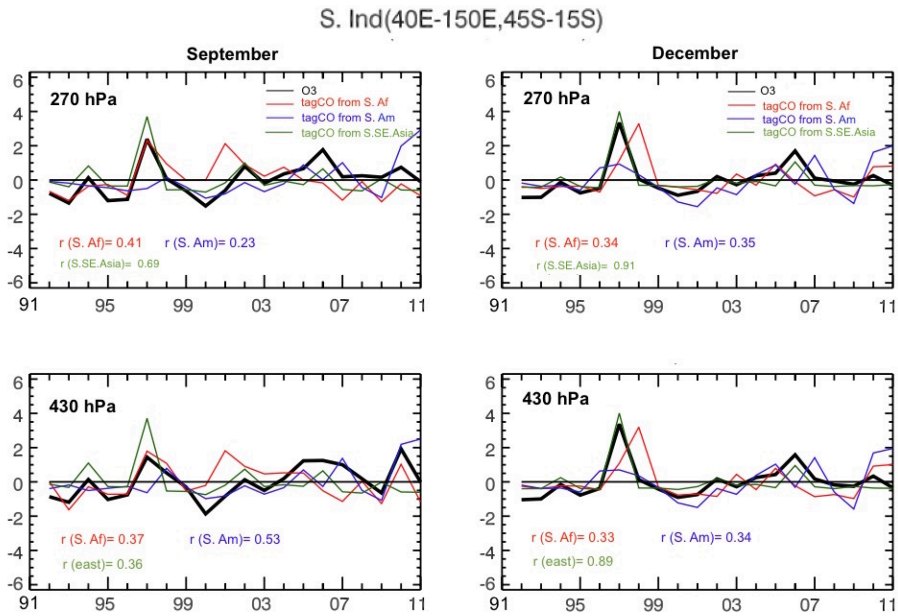

Figure 12: The standardized anomalies of the tagged CO tracers over South Indian Ocean region from three burning source regions, including southern Africa (red), South America (blue) and South and Southeast Asia (green) and their comparison with the EmissO_3 (black) at 270 and 430 hPa in September and December from 1992 to 2011.

Junhua Liu 1/15/2017 2:57 PM
Deleted: 1

Junhua Liu 12/31/2016 7:59 AM
Deleted: Eastern region

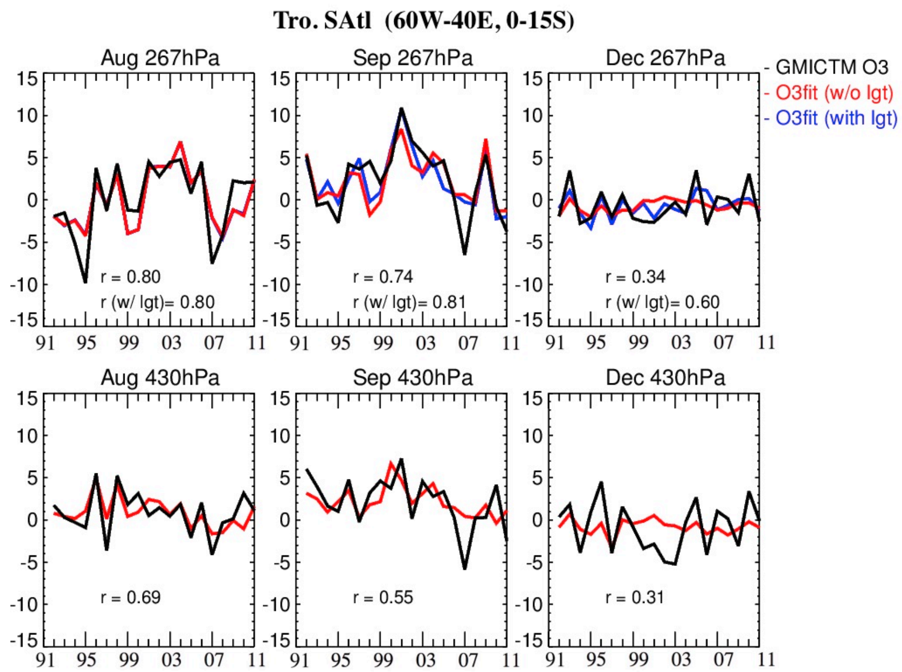

Figure 13: Comparison of the simulated ozone anomalies and the reconstructed ozone anomalies relying on two predictor variables: StratO$_3$, EmissO$_3$ (red) over Tropical South Atlantic region at 270 hPa and 430 hPa. At 270 hPa, the reconstructed ozone anomalies from three predictor variables including lightning NO$_X$ (blue) are added. Three panels show results from August (left), September (middle) and December (right) from 1992 to 2011. Unit for y-axis is ppb.

Junhua Liu 1/15/2017 2:57 PM
Deleted: 2

Junhua Liu 2/2/2017 1:54 PM
Formatted: Font:Underline color: Auto, Font color: Auto

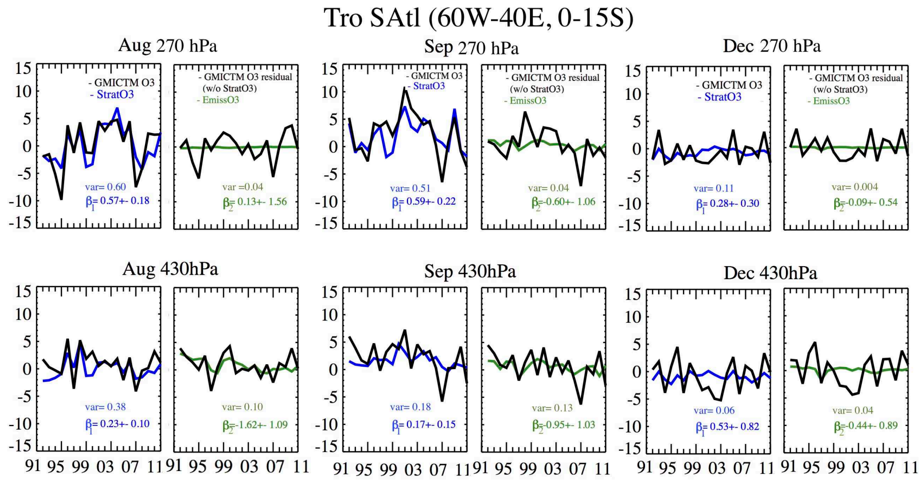

Figure 14: The multi-regression results of simulated ozone anomalies over tropical South Atlantic region relying on StratO$_3$ (blue), EmissO$_3$ (green) at 270 hPa and 430 hPa. Three panels show results from August (left), September (middle) and December (right) from 1992 to 2011. Each panel contains two columns. The left column of each panel compares the anomalies of StratO$_3$ (blue) and simulated ozone mixing ratio (black) from the GMI-CTM model at 270 and 430 hPa. The right column compares the simulated O$_3$ residual after removing the regression from StratO$_3$ (black line) and EmissO$_3$ (green line) at these two levels. EmissO$_3$ is calculated from the difference of simulated ozone between the run with yearly-varied emission and the run with constant emission. Unit for y-axis is ppb. The variance explained by each predictor (var), regression coefficient (β) and its 95% confidence level are labeled in each panel

Junhua Liu 1/15/2017 2:57 PM
Deleted: 3

Junhua Liu 1/15/2017 12:40 PM
Deleted: correlation (r),

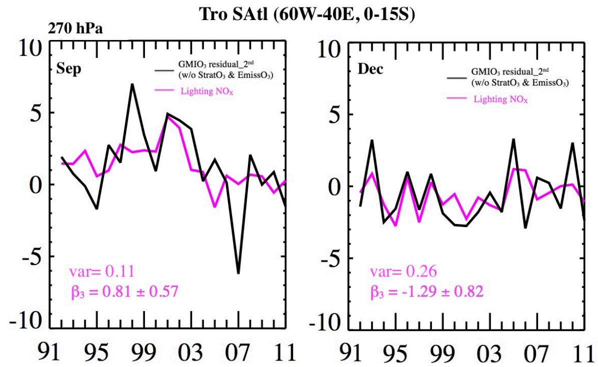

Figure 15: The comparison between regression of lightning NO_X (magenta) and the ozone residual after removing the regression of StratO3 and $EmissO_3$ (black) at 270 hPa in September (left) and December (right) over tropical South Atlantic region. The increased variance explained by the regression by adding lightning NO_X (var), regression coefficient (β) and its 95% confidence level are labeled in each panel.

Junhua Liu 1/15/2017 2:57 PM
Deleted: 4

Junhua Liu 1/15/2017 12:50 PM
Deleted: correlation (r),

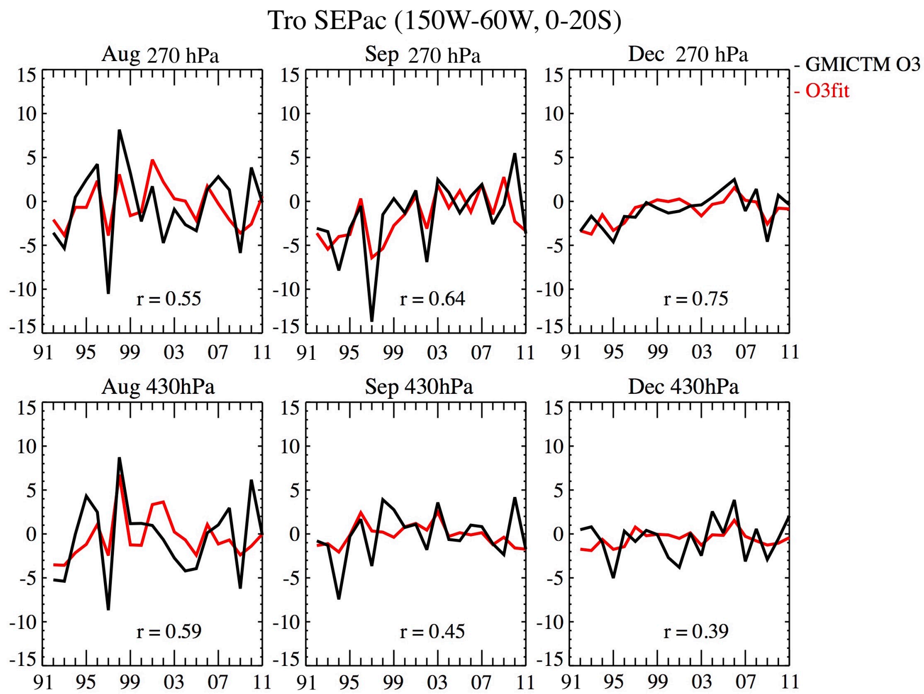

Figure 16: Comparison of the simulated ozone anomalies and the reconstructed ozone anomalies relying on two predictor variables: $StratO_3$, $EmissO_3$ at 270 hPa and 430 hPa over Tropical southeastern Pacific. Three panels show results from August (left), September (middle) and December (right) from 1992 to 2011. Unit for y-axis is ppb.

Junhua Liu 1/15/2017 2:58 PM
Deleted: 5

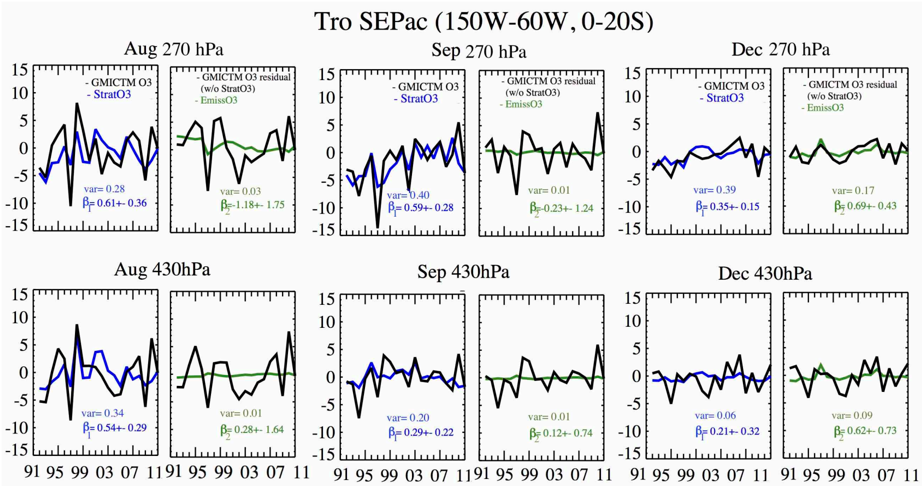

Figure 17: The multi-regression results of simulated ozone anomalies over tropical southeastern Pacific region relying on two predictor variables: $StratO_3$ (blue), $EmissO_3$ (green) at 270 hPa and 430 hPa. Three panels show results from August (left), September (middle) and December (right) from 1992 to 2011. Each panel contains two columns. The left column of each panel compares the anomalies of $StratO_3$ (blue) and simulated ozone mixing ratio (black) from the GMI-CTM model at 270 and 430 hPa. The right column compares the simulated O_3 residual after removing the regression from $StratO_3$ (black line) and $EmissO_3$ (green line) at these two levels. $EmissO_3$ is calculated from the difference of simulated ozone between the run with yearly-varied emission and the run with constant emission. Unit for y-axis is ppb. The variance explained by each predictor (var), regression coefficient (β) and its 95% confidence level are labeled in each panel.

Junhua Liu 1/15/2017 2:58 PM
Deleted: 6

Junhua Liu 1/15/2017 12:40 PM
Deleted: correlation (r),

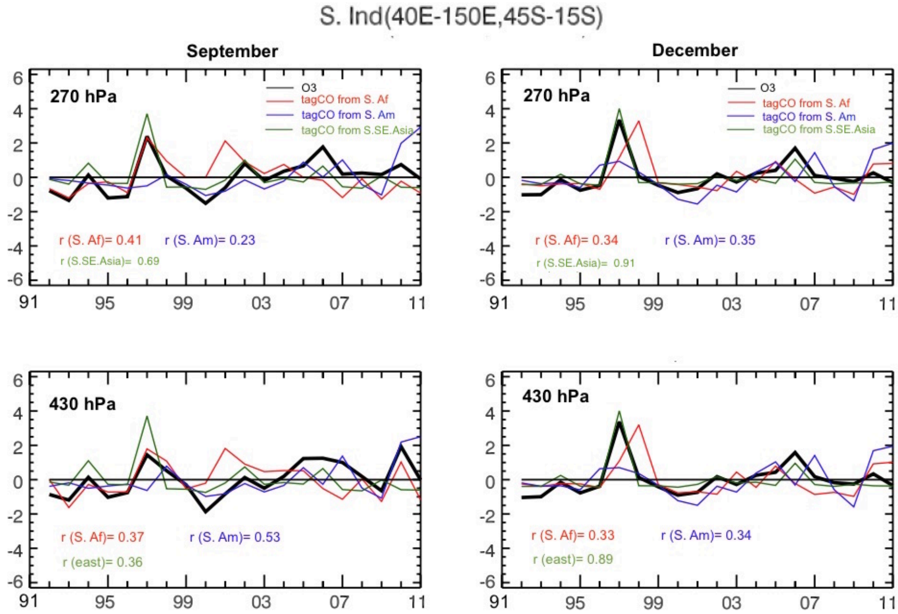

Figure 18: The standardized anomalies of the tagged CO tracers over tropical southeastern Pacific region from three burning regions, including southern Africa (red), South America (blue) and South and Southeast Asia (green) and their comparison with the EmissO3 (black) at 270 and 430 hPa in September from 1992 to 2011.

Junhua Liu 1/15/2017 2:58 PM
Deleted: 7

Junhua Liu 12/31/2016 7:59 AM
Deleted: Eastern region

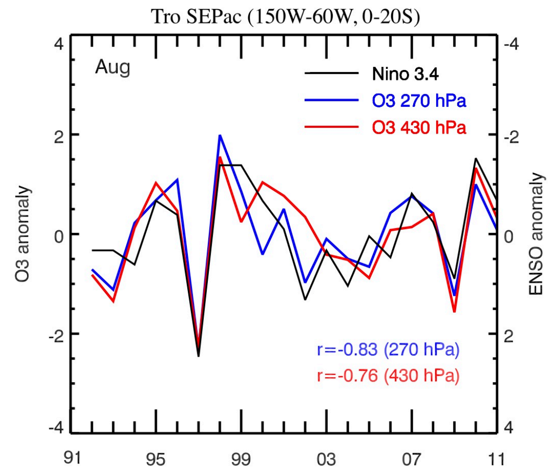

Figure 19: Comparison of IAV of ozone anomalies over tropical southeastern Pacific region at 270 hPa (blue) and 430 hPa (red) with Niño 3.4 index in August from 1992 to 2011. The 2nd y-axis for the ENSO anomaly is reversed.

Junhua Liu 1/15/2017 2:58 PM
Deleted: 8